

Qudits and high-dimensional quantum computing

Yuchen Wang¹, Zixuan Hu¹, Barry C. Sanders*², and Sabre Kais^{†1}

¹Department of Chemistry, Department of Physics and Purdue Quantum Science and Engineering Institute, Purdue University, West Lafayette, Indiana 47907, USA

²Institute for Quantum Science and Technology, University of Calgary, Alberta T2N 1N4, Canada

March 31, 2022

Abstract

Qudit is a multi-level computational unit alternative to the conventional 2-level qubit. Compared to qubit, qudit provides a larger state space to store and process information, and thus can provide reduction of the circuit complexity, simplification of the experimental setup and enhancement of the algorithm efficiency. This review provides an overview of qudit-based quantum computing covering a variety of topics ranging from circuit building, algorithm design, to experimental methods. We first discuss the qudit gate universality and a variety of qudit gates including the $\pi/8$ gate, the SWAP gate, and the multi-level controlled-gate. We then present the qudit version of several representative quantum algorithms including the Deutsch-Jozsa algorithm, the quantum Fourier transform, and the phase estimation algorithm. Finally we discuss various physical realizations for qudit computation such as the photonic platform, ion trap, and nuclear magnetic resonance.

1 Introduction to qudits

Qudit technology, with a qudit being a quantum version of d -ary digits for $d > 2$ [1], is emerging as an alternative to qubits for quantum computation and quantum information science. Due to its multi-level nature, qudit provides a larger state space to store and process information and the ability to do multiple control operations simultaneously [2]. These features play an important role in the reduction of the circuit complexity, the simplification of the experimental setup and the enhancement of the algorithm efficiency [3, 4, 5, 2]. The advantage

*sandersb@ucalgary.ca

†kais@purdue.edu

of the qudit not only applies to the circuit model for quantum computers but also applies to adiabatic quantum computing devices [6, 7], topological quantum systems [8, 9, 10] and more. The qudit-based quantum computing system can be implemented on various physical platforms such as photonic systems [2, 11], continuous spin systems [12, 13], ion trap [14], nuclear magnetic resonance [15, 16] and molecular magnets [17].

Although the qudit systems advantages in various applications and potentials for future development are substantial, this system receives less attention than the conventional qubit-based quantum computing, and a comprehensive review of the qudit-based models and technologies is needed. This review article provides an overview of qudit-based quantum computing covering a variety of topics ranging from circuit building [18, 19, 20, 21, 22], algorithm design [16, 23, 24, 13, 25, 26, 27], to experimental methods [2, 11, 12, 13, 14, 15, 16, 17]. In this article, high-dimensional generalizations of many widely used quantum gates are presented and the universality of the qudit gates is shown. Qudit versions of three major classes of quantum algorithms—algorithms for the oracles decision problems (e.g., the Deutsch-Jozsa algorithm [23]), algorithms for the hidden non-abelian subgroup problems (e.g. the phase-estimation algorithms (PEAs) [25]) and the quantum search algorithm (e.g. the Grover's algorithm [27])—are discussed and the comparison of the qudit designs versus the qubit designs is analyzed. Finally, we introduce various physical platforms that can implement qudit computation and compare their performances with their qubit counterparts.

Our article is organized as follows. Definitions and properties of a qudit and related qudit gates are given in §2. The generalization of the universal gate set to qudit systems and several proposed sets are provided in §2.1. Then §2.2 lists various examples of qudit gates and discusses the difference and possible improvement of these gates over their qubit counterparts. A discussion of the gate efficiency of synthesizing an arbitrary unitary U using geometric method is given in §2.3. The next section, §3, provides an introduction to qudit algorithms: a single-qudit algorithm that finds the parity of a permutation in §3.1.1, the Deutsch-Jozsa algorithm in §3.1.2, the Bernstein-Vazirani algorithm in §3.1.3, the quantum Fourier transform in §3.2.1, the PEA in §3.2.2 and the quantum search algorithm in §3.3. In §4, we provide various realizations of the qudit algorithms on physical platforms and discuss their applications. We discuss possible improvements in computational speed-up, resource saving and implementations on physical platforms. A qudit with a larger state space than a qubit can utilize the full potential of physical systems such as photon in §4.1, ion trap in §4.2, nuclear magnetic resonance in §4.3 and molecular magnet in §4.4. Finally, we give a summary of the qudit systems and provide our perspective for the future developments and applications of the qudit in §5.

2 Quantum gates for qudits

A *qudit* is a quantum version of d -ary digits whose state can be described by a vector in the d dimensional Hilbert space \mathcal{H}_d [1]. The space is spanned by a set of orthonormal basis vectors $\{|0\rangle, |1\rangle, |2\rangle, \dots, |d-1\rangle\}$. The state of a qudit has the general form

$$|\alpha\rangle = \alpha_0 |0\rangle + \alpha_1 |1\rangle + \alpha_2 |2\rangle + \dots + \alpha_{d-1} |d-1\rangle = \begin{pmatrix} \alpha_0 \\ \alpha_1 \\ \alpha_2 \\ \vdots \\ \alpha_{d-1} \end{pmatrix} \in \mathbb{C}^d \quad (1)$$

where $|\alpha_0|^2 + |\alpha_1|^2 + |\alpha_2|^2 + \dots + |\alpha_{d-1}|^2 = 1$. Qudit can replace qubit as the basic computational element for quantum algorithms. The state of a qudit is transformed by qudit gates.

This section gives a review of various qudit gates and their applications. §2.1 provides criteria for the qudit universality and introduces several fundamental qudit gate sets. §2.2 presents examples of qudit gates and illustrates their advantages compared to qubit gates. In the last section, §2.3, a quantitative discussion of the circuit efficiency is included to give a boundary of the number of elementary gates needed for decomposing an arbitrary unitary matrix.

2.1 Criteria for universal qudit gates

This subsection describes the universal gates for qudit-based quantum computing and information processing. We elaborate on the criteria for universality in §2.1.1 and give examples in §2.1.2.

2.1.1 Universality

In quantum simulation and computation, a product of matrices $U_k \in U(d^n)$ from some fixed set called the universal quantum gate set can be used to approximate any arbitrary unitary transformation U of the Hilbert space $\mathcal{H}_d^{\otimes n}$ with necessary precision in some appropriate norm [28]. This idea of *universality* not only applies to the qubit systems [29], but can also be extended to the qudit logic [30, 19, 31, 32, 33, 34]. Several discussions of standards and proposals for a universal qudit gate set exist. Vlasov shows that any unitary $U \in U(d^n)$ can be simulated with arbitrary precision using two specific noncommuting single qudit operations complemented by a two-qudit interaction operation [28]. Qudit gates can themselves be reduced to, and thus simulated by, sequences of qudit gates of lower-dimensional qudit gates [35, 36] Brylinski and Brylinski prove necessary and sufficient criteria for exact qudit universality which needs arbitrary single qudit gates complemented by one entangling two-qudit gate [1]. Exact universality implies that any unitary gate and any quantum process can be simulated with zero error. Neither of these methods is constructive and includes a method for physical implementation. Muthukrishnan and Stroud give

a constructive procedure for an exact simulation of an arbitrary unitary gate acting on N qudits using single- and two-qudit gates [37]. They use the spectral decomposition of unitary transformations and involve a gate library consisting of a family of continuous parameter gates. Brennen et al. identify criteria for exact quantum computation in qudit that relies on the QR decomposition of unitary transformations [38]. They use a gate library generated by a fixed set of single qudit Hamiltonians and a one parameter singly controlled phase gate as the components of the universal set. Implementing the concept of a coupling graph, they are able to show that universal computation is possible if the nodes (equivalently logical basis states) are connected.

2.1.2 Examples of universal gate sets

An explicit and physically realizable universal set comprising one-qudit general rotation gates and two-qudit controlled extensions of rotation gates is explained in this section [3]. We first define

$$U_d(\boldsymbol{\alpha}) : \sum_{l=0}^{d-1} \alpha_l |l\rangle \mapsto |d-1\rangle, \quad \boldsymbol{\alpha} := (\alpha_0, \alpha_1, \dots, \alpha_{d-1}). \quad (2)$$

as a d -dimensional transformation that maps a general qudit state to $|d-1\rangle$. Complex parameters of U_d may not be unique and have been addressed with probabilistic quantum search algorithm [37]. Here in this scheme, U_d can be deterministically decomposed into $d-1$ unitary transformations such that

$$U_d = X_d^{(d-1)}(a_{d-1}, b_{d-1}) \cdots X_d^{(1)}(a_1, b_1), \quad a_l := \alpha_l, \quad b_l := \sqrt{\sum_{i=0}^{l-1} \alpha_i^2} \quad (3)$$

with

$$X_d^{(l)}(x, y) = \begin{pmatrix} \mathbb{1}_{l-1} & & & \\ & \frac{x}{\sqrt{|x|^2+|y|^2}} & \frac{-y}{\sqrt{|x|^2+|y|^2}} & \\ & \frac{y^*}{\sqrt{|x|^2+|y|^2}} & \frac{x^*}{\sqrt{|x|^2+|y|^2}} & \\ & & & \mathbb{1}_{d-l-1} \end{pmatrix}. \quad (4)$$

The d -dimensional phase gate is

$$Z_d(\theta) := \sum_{l=0}^{d-1} e^{i(1-\text{sgn}(d-1-l))\theta} |l\rangle \langle l|, \quad (5)$$

which alters the phase of $|d-1\rangle$ by θ without affecting other states in the qudit, and sgn denotes the sign function.

Each primitive gate (such as $X_d^{(l)}$ or Z_d) can be implemented by controlling no more than two complex parameters (x, y in the $X_d^{(l)}$ gate and θ in the Z_d gate). Let R_d represents either $X_d^{(l)}$ or Z_d , then the controlled-qudit gate is

$$C_2[R_d] := \begin{pmatrix} \mathbb{1}_{d^2-d} & \\ & R_d \end{pmatrix}, \quad (6)$$

which is a $d^2 \times d^2$ matrix that acts on two qudits. R_d acts on d substates $|d-1\rangle|0\rangle, \dots, |d-1\rangle|d-1\rangle$, and the identity operation $\mathbb{1}_{d^2-d}$ acts on the remaining substates.

Now we work on an $N = d^n$ dimensional unitary transformation $U \in SU(d^n)$ acting on the n -qudit state. The sufficiency of the gates $X_d^{(l)}, Z_d$ and $C_2[R_d]$ to construct an arbitrary unitary transformation of $SU(d^n)$ is proved in three steps. The first step is the eigen-decomposition of U . From the representation theory, the unitary matrix U with N eigenvalues $\{\lambda_s\}$ and eigenstates $|E_s\rangle$ can be rewritten as

$$U = \sum_{j=1}^N e^{i\lambda_j} |E_j\rangle \langle E_j| = \prod_{j=1}^N \Upsilon_j \quad (7)$$

with eigenoperators

$$\Upsilon_j = \sum_{s=1}^N e^{i(1-|\text{sgn}(j-s)|)\lambda_s} |E_s\rangle \langle E_s|. \quad (8)$$

Then the eigenoperators can be synthesized with two basic transformations as [37]

$$\Upsilon_j = U_{j,N}^{-1} Z_{j,N} U_{j,N}. \quad (9)$$

Here $U_{j,N}$ and $Z_{j,N}$ are the N -dimensional analogues of U_d and Z_d such that $U_{j,N}$ transforms the j th eigenstate to $|N-1\rangle$ and $Z_{j,N}$ changes the phase of $|N-1\rangle$ with the j th eigenphase λ_j , leaving other computation states unchanged. According to Eq. (3), $U_{j,N}$ can be decomposed with primitive gates $X_{j,N}^{(l)}(x, y)$. Thus, $X_{j,N}(x, y)$ and $Z_{j,N}$ are sufficient to decompose U .

The second step is to realize the decomposition of $U_{j,N}$ and $Z_{j,N}$. In other words, $U_{j,N}$ and $Z_{j,N}$ need to be decomposed in terms of multi-qudit-controlled gates. For convenience denote $C_m[R_d]$ as

$$C_m[R_d] = \begin{pmatrix} \mathbb{1}_{d^m-d} & \\ & R_d \end{pmatrix}, \quad (10)$$

which acts on the d^m -dimensional computational basis of m -qudit space. It is proved in the appendix of Ref. [3] that each $U_{j,N}$ can be decomposed into some combinations of $C_m[R_d]$ and $C_m[P_d(p, q)]$ where $P_d(p, q)$ is the permutation of $|p\rangle$ and $|q\rangle$ state. The third step is using the two-qudit gates $C_2[R_d]$ and $C_2[P_d(p, q)]$ to complete the primitive decomposition of $C_m[R_d]$. One possible decomposition is illustrated in Fig. 1 for $d > 2$. This circuit uses $r = \lceil (m-2)/(d-2) \rceil$ auxiliary qudits ($\lceil x \rceil$ denotes the smallest integer greater than x). The last box contains $R_d = Z_d$ or $X_d^{(l)}$. $C_m[R_d]$ is implemented with these gates combined. All of the three steps together prove that the qudit gates set

$$\Gamma_d := \{X_d^{(l)}, Z_d, C_2[R_d]\} \quad (11)$$

is universal for the quantum computation using qudit systems.

The total number of primitive operations in this decomposition method is

$$L \leq 2N \times 3d^{n-1} \times n \times (d-2) + N \times n \leq 6nd^{2n} + nd^n \quad (12)$$

for a general n -qudit unitary operation. One advantage of this qudit model (compared to the qubit model) is a reduction of the number of qudits needed to span the quantum memory. To explain this, we need at least $n_1 = \log_2 N$ qubits to represent an N -dimensional system in qubits while in qudits we need $n_2 = \log_d N$ qudits. The qudit system has a reduction factor $k = n_1/n_2 = \log_2 d$. The other advantage is these primitive qudit gates can be easily implemented with fewer free parameters [3].

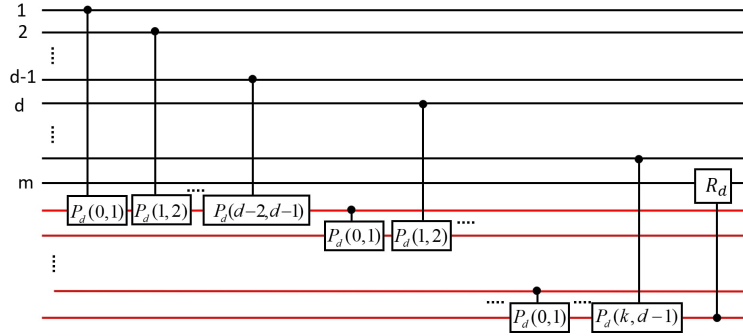


Figure 1: The schematic circuit of $C_m[R_d]$ with $C_2[R_d]$ and $C_2[P_d(p, q)]$. The horizontal lines represent qudits, with the red lines denoting the auxiliary qudits being initialized to $|0\rangle$ and the black lines denoting m controlling qudits. Vertical lines represent the two-qudit controlled gates, originating from the control qudit (which is required to be in $|0\rangle$ for the gate to apply) and terminating in a box on the target qudit. $P_d(p, q)$ is the permutation of $|p\rangle$ and $|q\rangle$ state, and R_d is either $X_d^{(l)}$ or Z_d .

For qudit quantum computing, depending on the implementation platform, other universal quantum gate sets can be considered. For example, in a recent proposal for topological quantum computing with metaplectic anyons, Cui and Wang prove a universal gates set for qutrit and *qupit* systems, for a qupit being a qudit with p dimensions and p is an odd prime number larger than 3 [8]. The proposed universal set is a qudit analogy of the qubit universal set and it consists several generalized qudit gates from the universal qubit set.

The generalized Hadamard gate for qudits H_d is

$$H_d |j\rangle = \frac{1}{\sqrt{d}} \sum_{i=0}^{d-1} \omega_d^{ij} |i\rangle, j+1 \in [d] := \{1, \dots, d\}, \quad (13)$$

where

$$\omega := e^{2\pi i/d}. \quad (14)$$

A natural generalization of the CNOT gate is the following SUM gate

$$\text{SUM}_d |i, j\rangle = |i, i + j(\text{mod } d)\rangle, i + 1, j + 1 \in [d]. \quad (15)$$

The $\pi/8$ gate is the 4th root of the Pauli σ_z matrix. The σ_z can be generalized to $Q[i]$ gates for qudits,

$$Q[i]_d |j\rangle = \omega_d^{\delta_{ij}} |j\rangle, \quad (16)$$

with ω defined by Eq. (14) and the related $P[i]$ gates are

$$P[i]_d |j\rangle = (-\omega_d^2)^{\delta_{ij}} |j\rangle, \quad i + 1, j + 1 \in [d]. \quad (17)$$

When $d = 3$, the $P[i]$ gate is a square root of the $Q[i]$ gate and in general, when p is an odd prime, $Q[i]_p$ is always a power of $P[i]_p$.

The proposed gate set for the qutrit system is the Hadamard gate H_3 , the sum gate SUM_3 and any gate from the set $\{P[0]_3, P[1]_3, P[2]_3\}$. This set has a strong analogy with the standard qubit universal set $\{\text{CNOT}, H, T = \pi/8\text{-gate}\}$ in that the qutrit set generate the qutrit Clifford group whereas the qubit set generate the qubit Clifford group (the definition of the Clifford group can be found in §2.2.1). Whereas the rigorous proof can be found in Ref. [8], the proving process follows the idea introduced in Ref. [1] that the gate SUM_3 is imprimitive, and the Hadamard H_3 and any gate from $\{P[0]_3, P[1]_3, P[2]_3\}$ generates a dense subgroup of $SU(3)$. Similarly, the proposed gate set for the qupit system is the Hadamard gate H_p , the sum gate SUM_p and the gates $Q[i]_p$ for $i \in [p-1]$. Note that the gate $Q[0]_p$ can be constructed from $Q[i]_p, i \in [p-1]$. The proof is analogous to that of the qutrit set. The Hadamard H_p and the $Q[i]$ gates generate a dense subgroup of $SU(p)$ and SUM_p is an imprimitive gate. Implementing Theorem 1.3 in Ref. [1], the set is a universal gate set. These universal gate sets for the qudit systems, with fewer numbers of gates in each set compare to that in the previous examples, have the potential to perform qudit quantum algorithms on the topological quantum computer.

2.2 Examples of qudit gates

In this section we introduce the qudit versions of many important quantum gates and discuss some of the gates' advantages compared to their qubit counterparts. The gates discussed are the qudit versions of the $\pi/8$ gate in §2.2.1, the SWAP gate in §2.2.2 and the multi-level controlled gate in §2.2.4. in §2.2.3, we also introduce how to simplify the qubit Toffoli gate by replacing one of the qubit to qudit. This gives ideas about improving the qubit circuits and gates by introducing qudits to the system.

2.2.1 Qudit versions $\pi/8$ gate

The qubit $\pi/8$ gate T has an important role in quantum computing and information processing. The reason behind this gate's wide range of applications is its close relationship with the Clifford group, while still not being a member of

the group. From the Gottesman-Knill theorem [39] it is shown that a circuit using only Clifford gates and Pauli measurements is insufficient for universal quantum computation (UQC). The $\pi/8$ gate, which is non-Clifford and from the third level of the Clifford hierarchy, is the essential gate to obtaining UQC [40]. This gate can be generalized to a d dimensional qudit system, where, throughout the process, d is assumed to be a prime number greater than 2 [18].

To define the Clifford group for a d -dimensional qudit space, we first define the Pauli Z gate and Pauli X gate. The Pauli Z gate and Pauli X gate are generalized to d dimension in the matrix forms [41, 42, 12, 43]

$${}^dX = \begin{pmatrix} 0 & 0 & \cdots & 0 & 1 \\ 1 & 0 & \cdots & 0 & 0 \\ 0 & 1 & \cdots & 0 & 0 \\ \vdots & \vdots & \ddots & \vdots & \vdots \\ 0 & 0 & \cdots & 1 & 0 \end{pmatrix}, {}^dZ = \begin{pmatrix} 1 & 0 & 0 & \cdots & 0 \\ 0 & \omega & 0 & \cdots & 0 \\ 0 & 0 & \omega^2 & \cdots & 0 \\ \vdots & \vdots & \vdots & \ddots & \vdots \\ 0 & 0 & 0 & \cdots & \omega^{d-1} \end{pmatrix} \quad (18)$$

for ω the d^{th} root of unity (14). The function of the Z gate is adding different phase factors to each basis states and that of the X gate is shifting the basis state to the next following state. Using basis states the two gates are

$$Z|j\rangle := \omega^j|j\rangle \quad X|j\rangle := |j+1\rangle, \quad j \in \{0, 1, 2, \dots, d-1\}. \quad (19)$$

In general, products of the Pauli operators are called displacement operators,

$$D_{(x|z)} = \tau^{xz} X_d^x Z_d^z, \quad \tau := e^{(d+1)\pi i/d} = \omega^{2^{-1}}. \quad (20)$$

This leads to the definition of the Weyl-Heisenberg group (or the generalized Pauli group) for a single qudit as [41, 42, 12, 43]

$$\mathcal{G} = \{\tau^c D_{\vec{\chi}} | \vec{\chi} \in \mathbb{Z}_d^2, c \in \mathbb{Z}_d\} \quad (\mathbb{Z}_d = \{0, 1, \dots, d-1\}), \quad (21)$$

where $\vec{\chi}$ is a two-vector with elements from \mathbb{Z}_d . With these preliminary concepts defined in Eqs. (18) through (21), we now define the Clifford group as the following: the set of the operators that maps the Weyl-Heisenberg group onto itself under conjugation is called the *Clifford group* [43, 44],

$$\mathcal{C} = \{C \in U(d) | C\mathcal{G}C^\dagger = \mathcal{G}\}. \quad (22)$$

A recursively defined set of gates, the so-called Clifford hierarchy, was introduced by Gottesman and Chuang as

$$\mathcal{C}_{k+1} = \{U|UC_1U^\dagger \subseteq \mathcal{C}_k\}, \quad (23)$$

for \mathcal{C}_1 the Pauli group [45]. The sets $\mathcal{C}_{k \geq 3}$ do not form groups, although the diagonal subsets of \mathcal{C}_3 , which is our focus here, do form a group.

The explicit formula for building a Clifford unitary gate with

$$F = \begin{pmatrix} \alpha & \beta \\ \gamma & \delta \end{pmatrix} \in \text{SL}(2, \mathbb{Z}_d), \quad \vec{\chi} = \begin{pmatrix} x \\ z \end{pmatrix} \in \mathbb{Z}_d^2 \quad (24)$$

is

$$C_{(F|\bar{\chi})} = D_{(x|z)} V_F, \quad (25)$$

$$V_F = \begin{cases} \frac{1}{\sqrt{d}} \sum_{j,k=0}^{d-1} \tau^{\beta^{-1}(\alpha k^2 - 2jk + \delta j^2)} |j\rangle \langle k|, & \beta \neq 0 \\ \sum_{k=0}^{d-1} \tau^{\alpha \gamma k^2} |\alpha k\rangle \langle k|, & \beta = 0. \end{cases} \quad (26)$$

The special case $\beta = 0$ is particularly relevant to the later derivation, and

$$\begin{aligned} \det \left(\sum_{k=0}^{d-1} \tau^{\alpha \gamma k^2} |k\rangle \langle k| \right) &= \tau^{\frac{\alpha \gamma}{6} (2d-1)(d-1)d}, \\ &= \begin{cases} \tau^{2\alpha \gamma}, & d = 3, \\ 1, & \forall d > 3, \end{cases} \end{aligned} \quad (27)$$

can be shown. In the $d = 3$ case, we use

$$C \left(\left(\begin{bmatrix} 1 & 0 \\ \gamma & 1 \end{bmatrix} \middle| \begin{bmatrix} x \\ z \end{bmatrix} \right) \right) \in SU(p) \quad \forall p > 3 \quad (28)$$

and

$$\det \left(C \left(\left(\begin{bmatrix} 1 & 0 \\ \gamma & 1 \end{bmatrix} \middle| \begin{bmatrix} x \\ z \end{bmatrix} \right) \right) \right) = \tau^{2\gamma} \quad \text{for } p = 3. \quad (29)$$

With all the mathematical definitions at hand, we are ready to give an explicit form of the qudit $\pi/8$ gate. For simplicity and in analogy with the qubit $\pi/8$ gate, we choose the qudit gate U_v to be diagonal in the computational basis. We claim that, for $d > 3$, U_v can be written in the form

$$U_v = U(v_0, v_1, \dots) = \sum_{k=0}^{d-1} \omega^{v_k} |k\rangle \langle k| \quad (v_k \in \mathbb{Z}_d). \quad (30)$$

A straightforward application of Eqs. (20) and (30) yields

$$U_v D_{(x|z)} U_v^\dagger = D_{(x|z)} \sum_k \omega^{v_{k+1} - v_k} |k\rangle \langle k|. \quad (31)$$

As U_v is to be a member of \mathcal{C}_3 , the right hand side of Eq. (31) must be a Clifford gate. We ignore the trivial case $U_v D_{(0|z)} U_v^\dagger = D_{(0|z)}$ and focus on the case $U_v D_{(1|0)} U_v^\dagger$ in order to derive an explicit expression for U_v .

We define $\gamma', z', \epsilon' \in \mathbb{Z}_d$ such that

$$U_v D_{(1|0)} U_v^\dagger = \omega^{\epsilon'} C \left(\left(\begin{bmatrix} 1 & 0 \\ \gamma' & 1 \end{bmatrix} \middle| \begin{bmatrix} 1 \\ z' \end{bmatrix} \right) \right) \quad (32)$$

From Eqs. (26) and (31) we see that the right-hand side of Eq. (32) is the most general form, and we note that $U \in SU(d)$ implies $\omega^{\gamma'} U \in SU(d)$, for

any integer k . We rewrite the left-hand side of Eq. (32) using Eq. (31) and right-hand side using Eq. (26) and obtain

$$D_{(1|0)} \sum_k \omega^{v_{k+1}-v_k} |k\rangle \langle k| = \omega^{\epsilon'} D_{(1|z')} \sum_{k=0}^{d-1} \tau^{\gamma' k^2} |k\rangle \langle k|. \quad (33)$$

After cancelling common factors of $D_{(1|0)}$, an identity between two diagonal matrices remains such that

$$\omega^{v_{k+1}-v_k} = \omega^{\epsilon'} \tau^{z'} \omega^{kz'} \tau^{\gamma' k^2} \quad (\forall k \in \mathbb{Z}_d), \quad (34)$$

or, equivalently, using Eq. (20),

$$v_{k+1} - v_k = \epsilon' + 2^{-1}z' + kz' + 2^{-1}\gamma'k^2. \quad (35)$$

From here, we derive the recursive relation

$$v_{k+1} = v_k + k(2^{-1}\gamma'k + z') + 2^{-1}z' + \epsilon'. \quad (36)$$

with a boundary condition $v_0 = 0$, Now we solve to obtain

$$v_k = \frac{1}{12}k\{\gamma' + k[6z' + (2k-3)\gamma']\} + k\epsilon', \quad (37)$$

where all factors are understood to be evaluated modulo d . For example, with $d = 5$, the fifth root of unity (14) is $\omega = e^{2\pi i/5}$ and choosing $z' = 1, \gamma' = 4$ and $\epsilon' = 0$, we obtain

$$v = (v_0, v_1, v_2, v_3, v_4) = (0, 3, 4, 2, 1) \quad (38)$$

so that

$$U_v = \begin{pmatrix} \omega^0 & 0 & 0 & 0 & 0 \\ 0 & \omega^{-2} & 0 & 0 & 0 \\ 0 & 0 & \omega^{-1} & 0 & 0 \\ 0 & 0 & 0 & \omega^2 & 0 \\ 0 & 0 & 0 & 0 & \omega^1 \end{pmatrix} \quad (39)$$

The powers of ω along the diagonal of U_v sum to zero modulo d and, consequently, $\det(U_v) = 1$.

For the $d = 3$ case, because of Eq. (27) extra work is needed for solving a matrix equation analogous to Eq. (32). First a global phase factor $e^{i\phi}$ is introduced so that

$$\det \left(e^{i\phi} \sum_{k=0}^{d-1} \tau^{\gamma k^2} |k\rangle \langle k| \right) = 1 \implies \phi = 4\pi\gamma/9. \quad (40)$$

The ninth root of unity (14) is $\omega = e^{2\pi i/9}$ and, from Eq. (29) we derive that

$$\det \left(\omega^{2\gamma'} C \left(\begin{bmatrix} 1 & 0 \\ \gamma' & 1 \end{bmatrix} \middle| \begin{bmatrix} 1 \\ z' \end{bmatrix} \right) \right) = 1. \quad (41)$$

The qudit version of $U_{\pi/8}$ has a more general form than in Eq. (30); i.e.

$$U_v = U(v_0, v_1, \dots) = \sum_{k=0}^2 \omega^{v_k} |k\rangle \langle k|, \quad v_k \in \mathbb{Z}_9. \quad (42)$$

A similar calculation as before leads to the general solution

$$v = (0, 6z' + 2\gamma' + 3\epsilon', 6z' + \gamma' + 6\epsilon') \pmod{9}. \quad (43)$$

For example, choosing $z' = 1, \gamma' = 2$ and $\epsilon' = 0$,

$$U_v = \begin{pmatrix} \omega^0 & 0 & 0 \\ 0 & \omega^1 & 0 \\ 0 & 0 & \omega^{-1} \end{pmatrix}. \quad (44)$$

The $\pi/8$ gate, with its close relation to the Clifford group has many applications and utilities in teleportation-based UQC [45], transversal implementation [46, 47], learning an unknown gate [48], or securing assisted quantum computation [49]. It is also notable that $\pi/8$ gate is remarkable due to its geometrical relationship with the set of Clifford gates it is the single-qubit unitary $U \in SU(2)$ that is farthest outside the convex hull of Clifford operations [18]. The generalized qudit version of the $\pi/8$ gate, U_v , is shown to be identical, up to an unimportant factor of a Clifford gate, to the maximally robust qudit gates for qudit fault-tolerant UQC discussed in reference [50]. This gate also plays an important role in the magic-state distillation (MSD) protocols for general qudit systems, which was first established for qutrits [51] and then extended to all prime-dimensional qudits [52].

2.2.2 Qudit SWAP gate

A SWAP gate is used to exchange the states of two qudit such that:

$$\text{SWAP}|\phi\rangle|\psi\rangle = |\psi\rangle|\phi\rangle \quad (45)$$

Various methods to achieve the SWAP gate use different variants of qudit controlled gates [53, 54, 55, 56, 57, 58, 59] as shown in Fig.2. The most used component of the SWAP gate is a controlled-shift gate CX_d that perform the following operation:

$$CX_d|x\rangle|y\rangle = |x\rangle|x+y\rangle \quad (46)$$

with a modulo d addition. Its inverse operation is

$$CX_d^\dagger|x\rangle|y\rangle = |x\rangle|y-x\rangle \quad (47)$$

In some approaches, the resulting circuits need to be completed with the operation

$$X_d|x\rangle = |d-x\rangle = |-x\rangle, \quad (48)$$

which outputs the modulo d complement of the input. These circuits are not as simple and intuitive as the qubit SWAP gate [56] because the qudit generalization of the CNOT gate is not Hermitian, i.e., $CX_d \neq CX_d^\dagger$.

One way towards a Hermitian qudit CNOT uses the GXOR gate

$$GXOR |x\rangle |y\rangle = |x\rangle |x - y\rangle. \quad (49)$$

Nevertheless, a SWAP circuit with this gate still needs an X_d correction [59] as shown in Fig. 3. A partial SWAP gate S_p [19] works on a hybrid system where $|i\rangle$ is a qudit of dimension d_c and $|j\rangle$ is a qudit of dimension d_t

$$S_p |i\rangle \otimes |j\rangle = \begin{cases} |j\rangle \otimes |i\rangle & \text{for } i, j \in \mathbb{Z}_{d_p} \\ |i\rangle \otimes |j\rangle & \text{otherwise} \end{cases} \quad (50)$$

where $d_p \leq d_{\min} = \min(d_c, d_t)$

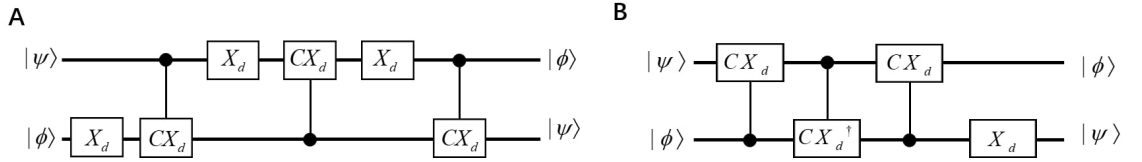


Figure 2: **(A)** is the qudit SWAP circuit using CX_d and X_d gates [56, 57]. **(B)** is the qudit SWAP circuits with the CX_d , the CX_d^\dagger and the X_d gates

In the rest of this section, we present a Hermitian qudit generalization of the CNOT gate with a symmetry configuration and describe a qudit SWAP circuit which only uses one type of qudit gate as shown in Fig. 4 **A** [20]. Compared with all the previously proposed SWAP gate for qudit, this method is easier to implement since there is only one type of gate $C\tilde{X}$ needed. To begin with, we define a gate $C\tilde{X}$ acting on d -level qudits $|x\rangle$ and $|y\rangle$ such that

$$C\tilde{X} |x\rangle |y\rangle = |x\rangle |-x - y\rangle, \quad (51)$$

where $|-x - y\rangle$ denotes a state $|i = -x - y\rangle$ in the range $i \in \{0, \dots, d - 1\} \bmod d$. Notice that, for $d = 2$, the $C\tilde{X}$ gate is equivalent to the CNOT gate. The SWAP gate for qudit can be built using three $C\tilde{X}$ gates and the evolution through the SWAP gate is

$$|x\rangle |y\rangle \xrightarrow{C\tilde{X}_{1,2}} |x\rangle |-x - y\rangle \quad (52)$$

$$|x\rangle |-x - y\rangle \xrightarrow{C\tilde{X}_{2,1}} |y\rangle |-x - y\rangle \quad (53)$$

$$|y\rangle |-x - y\rangle \xrightarrow{C\tilde{X}_{1,2}} |y\rangle |-y + x + y\rangle = |y\rangle |x\rangle \quad (54)$$

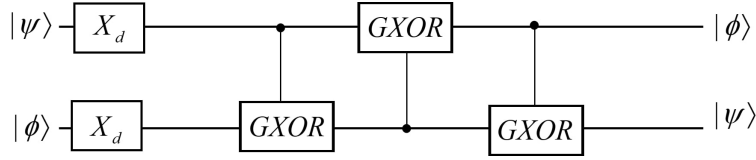


Figure 3: Qudit SWAP circuits with the $GXOR$ and the X_d gates.[58, 59]

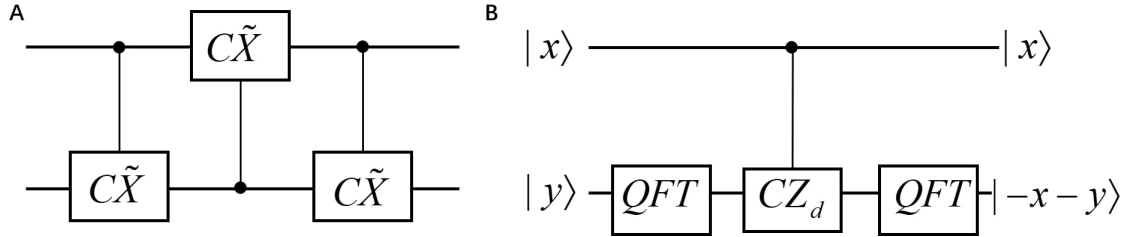


Figure 4: **(A)** is the qudit SWAP gate with the $C\tilde{X}$ gate. **(B)** is the decomposing $C\tilde{X}$ gate. The QFT represents the quantum Fourier transform while CZ_d is the selective phase shift gate.

$C\tilde{X}$ can be decomposed into three steps: two quantum Fourier transform operations(QFT) and the qudit generalization of the CZ gate as CZ_d . The circuit illustration for the sequence of these gates is shown in Fig. 4 **B**. The QFT takes any qudit state $|x\rangle$ into a uniform superposition

$$QFT |x\rangle = \frac{1}{\sqrt{d}} \sum_{k=0}^{d-1} e^{i2\pi xk/d} |k\rangle. \quad (55)$$

The CZ_d gate adds a phase to the target qudit depending on the state of the control qudit. Its effect on the input qudits is

$$CZ_d |x\rangle |y\rangle = e^{i2\pi xy/d} |x\rangle |y\rangle. \quad (56)$$

The inverse QFT undoes the Fourier transform process and the inverse of CZ_d is

$$CZ_d^\dagger |x\rangle |y\rangle = e^{-i2\pi xy/d} |x\rangle |y\rangle. \quad (57)$$

The total evolution of the desired $C\tilde{X}$ is shown as

$$|x\rangle|y\rangle \xrightarrow{QFT_2} \frac{1}{\sqrt{d}} \sum_{k=0}^{d-1} e^{i\frac{2\pi ky}{d}} |x\rangle|k\rangle \quad (58)$$

$$\xrightarrow{CZ_d} \frac{1}{\sqrt{d}} \sum_{k=0}^{d-1} e^{i\frac{2\pi ky}{d}} e^{i\frac{2\pi xk}{d}} |x\rangle|k\rangle = \frac{1}{\sqrt{d}} \sum_{k=0}^{d-1} e^{i\frac{2\pi k(x+y)}{d}} |x\rangle|k\rangle \quad (59)$$

$$\xrightarrow{QFT_2} \frac{1}{d} \sum_{l=0}^{d-1} \sum_{k=0}^{d-1} e^{i\frac{2\pi k(x+y)}{d}} e^{i\frac{2\pi kl}{d}} |x\rangle|l\rangle = |x\rangle|-x-y\rangle. \quad (60)$$

It is easy to show that $C\tilde{X}$ is its own inverse and then $C\tilde{X} = C\tilde{X}^\dagger$. For the proposed SWAP gate, both the QFT and CZ_d operations are realizable on a multilevel quantum systems. For example, there are implementations of them for multilevel atoms [37, 60]. The resulting SWAP gate provides a way to connect systems limited to the nearest-neighbour interactions. This gate provides a useful tool in the design and analysis of complex qudit circuits.

2.2.3 Simplified qubit Toffoli gate with a qudit

The Toffoli gate is well known for its application to universal reversible classical computation. In the field of quantum computing, the Toffoli gate plays a central role in quantum error correction [61], fault tolerance [62] and offers a simple universal quantum gate set combined with one qubit Hadamard gates [63]. In a qubit system, Toffoli gate is a three-qubit gate that flips the logical state of the target qubit conditional on the logical states of the two control qubits [64]. The simplest known qubit Toffoli gate, shown in Fig. 5, requires at least 5 two-qubit gates (6 if we restrict ourselves to only using CNOT gate) [65]. However, if the target qubit has a third level, i.e., a qutrit, the whole circuit can be achieved with three two-qubit gates [21].

A new qutrit gate X_a is introduced to the circuit that does the following: $X_a|0\rangle = |2\rangle$ and $X_a|2\rangle = |0\rangle$ with $X_a|1\rangle = |1\rangle$. The simplified circuit is shown in Fig. 6. The two controlled gates are the CNOT gate and a control-Z gate, which is achieved with a CNOT gate between two Hadamard gates. The Hadamard gate here operating on the qutrit is generalized from the normal Hadamard gate operating on a qubit—it only works with the $|0\rangle$ and $|1\rangle$, such that $H|0\rangle = 1/\sqrt{2}[|0\rangle+|1\rangle]$, $H|1\rangle = 1/\sqrt{2}[|0\rangle - |1\rangle]$ and $H|2\rangle = |2\rangle$. Comparing the circuit in Fig. 6 to that in Fig. 5, it is clear that the total number of gates is significantly reduced.

This method can be generalized to implement higher-order n -qubit-controlled Toffoli gates by utilizing a single $(n+1)$ -level target carrier during computation and using only $2n-1$ standard two-qubit gates [21]. In other words, for each extra control qubit we need an extra level in the target carrier. Compare $2n-1$ gates with the previous best known scheme, which requires $12n-11$ two-qubit gates and an extra overhead of $n-1$ extra ancilla qubits [65], this method offers a significant resource reduction. Furthermore, these schemes can be extended to

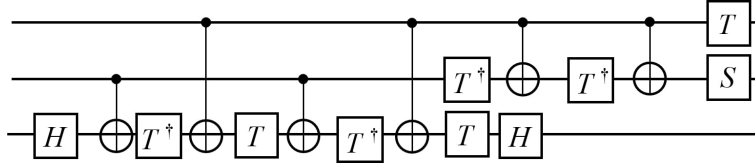


Figure 5: Decomposing qubit Toffoli gate with the universal qubit gates. H is the Hadamard gate, T is the $\pi/8$ gate and S is the phase gate.

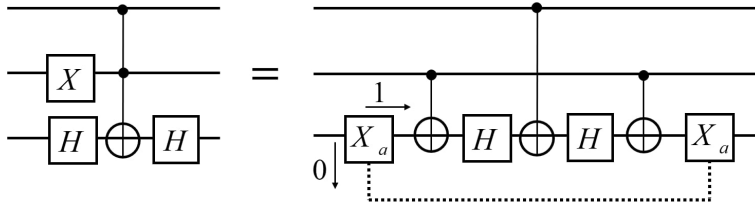


Figure 6: The Simplified Toffoli gate. The first two lines represent two control qubits and the third line represents a target qudit that has three accessible levels. Initially and finally, all of the quantum information is encoded in the $|0\rangle$ and $|1\rangle$ levels of each information carrier. The H is the generalized Hadamard gate such that $H|0\rangle = 1/\sqrt{2}[|0\rangle + |1\rangle]$, $H|1\rangle = 1/\sqrt{2}[|0\rangle - |1\rangle]$ and $H|2\rangle = |2\rangle$. X_a gate is a qudit gate such that $X_a|0\rangle = |2\rangle$ and $X_a|2\rangle = |0\rangle$ with $X_a|1\rangle = |1\rangle$. With the control being qubit, the target being qudit, the two qudit gate in this case is a hybrid gate.

more general quantum circuits such as the multi-qudit-controlled-unitary gate $C^n U$.

The previous method turns the target qubit into a qudit; another method simplifies the Toffoli gate by using only qudits and treating the first two levels of the qudit as qubit levels and other levels as auxiliary levels. The reduction in the complexity of Toffoli gate is accomplished by establishing a general relation between the dimensionality of qudits and their topology of connections for a scalable multi-qudit processor, where higher qudit levels are used for substituting ancillas [22].

Suppose we have a system of n qudits denoted as Q_i , $i \in \{1, \dots, n\}$ and each qudit has dimension $d_i \geq 2$. Qudits are initialized into pure or mix states on the first two levels, i.e., the qubit states, and zero population for the other levels, i.e., the auxiliary states. This scheme assumes the ability to perform single-qubit operations. We can apply the desirable unitary operation on the qubit states and leave the auxiliary states unchanged. We also assume that we have the ability to manipulate the auxiliary levels by a generalized inverting

gate X_m

$$X_m |0\rangle = |m\rangle, X_m |m\rangle = |0\rangle, X_m |y\rangle = |y\rangle, \text{ for } y \neq m, 0. \quad (61)$$

At the same time, the two-qubit CZ gates are applied corresponding to certain topology of physical connections between qudits. To determine this topology, a set E of ordered pairs (i, j) , such that $i, j \in \{1, \dots, n\}$, $i < j$, is introduced and the CZ gate is defined as

$$CZ |11\rangle_{Q_i, Q_j} = -|11\rangle_{Q_i, Q_j} \quad CZ |xy\rangle_{Q_i, Q_j} = |xy\rangle_{Q_i, Q_j} \text{ for } xy \neq 1, \quad (62)$$

with $x \in \{0, \dots, d_i - 1\}$ and $y \in \{0, \dots, d_j - 1\}$. The set E corresponds to the n -vertex-connected graph, i.e., a path exists between any pair of qudits. Let $\tilde{E} \subseteq E$ define an n -vertex connected acyclic graph known as a tree. The main result is: A strong reduction in the number of operations required for the realization of the n -qubit Toffoli gate is possible if

$$d_i \geq k_i + 1, \quad (63)$$

where d_i is the dimension of a qudit and the number k_i is the qudit's connections to other qudits within \tilde{E} . If this condition is fulfilled, then it is possible to realize the n -qubit Toffoli gate by employing $2n - 3$ two-qudit CZ gates. The detailed realization of the n -qubit Toffoli gate by the properties and special operations of the tree in topology can be found in Ref. [22]. The advantage of this scheme is the scalability and the ability to be further generalized for the implementation of multi-qubit controlled unitary gate $C^n U^{(t)}$.

These $C^n U$ gates are a crucial component in the PEA which underpins many important applications of quantum computing including quantum simulation [66] and the Shor's famous algorithm for factoring [67]. This idea of combining qudits of different dimensions or hybrid qudit gates can also be applied to other qudit gates such as the SWAP and SUM gates as shown in Ref. [19, 68]. Thus, introducing qudits into qubit systems to create a hybrid qudit system offers the potential of improvement to quantum computation.

2.2.4 Qudit multi-level controlled gate

For a qubit controlled gate, the control qubit has only two states so it is a "do-or-don't" gate. Qudits, on the other hand, have multiple accessible states and thus a qudit-controlled gate can perform a more complicated operation [69]. The *Muthukrishnan-Stroud gate* (MS gate) for a qudit applies the specified operation on the target qudit only if the control qudit is in a selected one of the d states, and leaves the target unchanged if the control qudit is in any other $d - 1$ states. Hence, the MS gate is essentially a "do-or-don't" gate generalized to qudits and does not fully utilize the d states on the control qudit [37].

To fully utilize the d states on the control qudit, people have developed the quantum multiplexer to perform the controlled U operations in a qudit system as shown in Fig. 7, where the MS gate and shifting gates are combined to apply

different operations to the target depending on different states on the control states [70]. Here we introduce the *multi-value-controlled gate (MVCG)* for qudits, which applies a unique operation to the target qudit for each unique state of the control qudit [2].

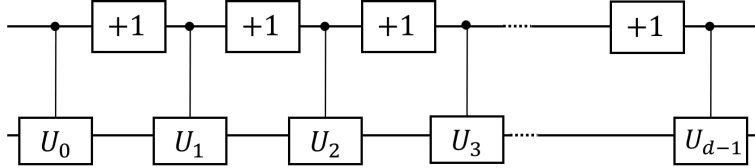


Figure 7: d -valued Quantum Multiplexer for the second qudit and its realization in terms of Muthukrishnan-Stroud gates (the control U operation that only act on one specific control state). The gate labeled $+1$ is the shifting gate that increases the state value of the control qudit by $1 \pmod{d}$. Depending on the value of the top control qudit, one of U_i is applied to the second qudit, for $i \in \{0, 1, \dots, d-1\}$.

For a d -dimensional qudit system, a two-qudit multi-value-controlled gate is represented by a $d^2 \times d^2$ matrix

$$MVCG = \begin{pmatrix} U_0 & 0 & 0 & \cdots & 0 \\ 0 & U_1 & 0 & \cdots & 0 \\ 0 & 0 & U_2 & \cdots & 0 \\ \vdots & \vdots & \vdots & \ddots & \vdots \\ 0 & 0 & 0 & \cdots & U_{d-1} \end{pmatrix}, \quad (64)$$

where each U_i ($i = 0, 1, \dots, d-1$) is a unique unitary single-qudit operation. The U_i operation is applied to the target qudit when the control qudit is in $|i\rangle$ state. In the later sections, §3.2.1 and §3.2.2 the controlled gates are *MVCG* and improve the efficiency of the qudit algorithm. *MVCG* can be built in many physical systems and one example in a photonic system is introduced in §4.1.

2.3 Geometrically quantifying qudit-gate efficiency

In a quantum computer, each qudit can remain coherent for a limited amount of time (decoherence time). After this time, the quantum information is lost due to the outside perturbations and noises. In the computation process, quantum gates take certain amount of time to alter the states of the qudits. The decoherence time of a qudit state limits the number of quantum gates in the circuit. Therefore, we need to design more efficient algorithms and circuits. A method exists to do a general systematic evaluation of the circuit efficiency with the mathematical techniques of Riemannian geometry [71]. By recasting the problem of finding quantum circuits as a geometric problem, we are able to suggest new quantum algorithms or to prove limitations on the power of

the quantum computers. This evaluation can be generalized to qutrit systems, where a lower bound for the number of gates needed to synthesize an arbitrary unitary operation is given [4].

To begin with, we assume that the operations done by the quantum circuit can be described by a unitary evolution U generated by some time-dependent Hamiltonian according to the Schrödinger equation $dU/dt = -iHU$ with the requirement that, at an appropriate final time t_f , $U(t_f) = U$. The difficulty of the computation can be characterized by a cost function $F[H(t)]$ on the Hamiltonian control $H(t)$ that defines a Riemannian geometry on the space of unitary operations [72]. Finding the optimal control function $H(t)$ for synthesizing a desired unitary U then corresponds to finding the minimal geodesics of the Riemannian geometry.

The minimal geodesic distance between the identity operation I and U is essentially equivalent to a lower bound to the number of gates required to synthesize U . Instead of Pauli matrices for the qubit representation of the Hamiltonian, the qutrit version of Hamiltonian is expanded in terms of the Gell-Mann matrices. Here we give an explicit form of the Gell-Mann matrices representation in d -dimension [5] which is used for qutrit (where $d = 3$) as well as other qudit systems in the later part of the section. Let e_{jk} denote the $d \times d$ matrix with a 1 in the (j, k) elements and 0s elsewhere, a basis can be described as

$$u_{jk}^d = e_{jk} + e_{kj}, \quad 1 \leq j < k \leq d, \quad (65)$$

$$u_{jk}^d = i(e_{jk} - e_{kj}), \quad 1 \leq k < j \leq d, \quad (66)$$

$$u_{jj}^d = \text{diag}(1, \dots, 1, -j, 0_{d-2j}), \quad j \in [d-1]. \quad (67)$$

Here, diag represents the diagonal matrix, 0_{d-2j} denotes the zeros of length $d - 2j$. u_{jk}^d are traceless and Hermitian and together with the identity matrix $\mathbf{1}_d$ span the vector space of $d \times d$ Hermitian matrix. These generalized Gell-Mann matrices construct one group representation of $SU(d)$ and other representations can be obtained by arbitrary unitary transformations. To derive the bases of $SU(d^n)$, we first define $x_l = u_{jk}^d$ with $l = jd + k, l \in [d^2]$ and

$$X_l^s = I^{\otimes s-1} \otimes x_l \otimes I^{\otimes d-s} \quad (68)$$

be an operator acting on the s -th qudit with x_l and the rest of the qudits with identity operation. The bases of $SU(d^n)$ is constructed by $\{Y_t^{P_t}\}, t \in [n], P_t = \{i_1, \dots, i_t\}$ with all possible $1 < i_1 < \dots < i_k < n$, where

$$Y_t^{P_t} = \prod_{k=1}^t X_{j_k}^{i_k}. \quad (69)$$

Y_t^P denotes all operators with generalized Gell-Mann matrices x_{j_1}, \dots, x_{j_k} acting on t qudits at sites $P = \{i_1, \dots, i_k\}$, respectively, and rest with identity. It is easy to prove that with the generalized Gell-Mann matrices representations, all 3-body interactions can be generated by 1-body and 2-body interactions.

Now the Hamiltonian in terms of the Gell-Mann matrices (with the notation σ) can be written as

$$H = \sum_{\sigma}^{\prime} h_{\sigma} \sigma + \sum_{\sigma}^{\prime\prime} h_{\sigma} \sigma. \quad (70)$$

All coefficients h_{σ} are real and, in the first sum, σ ranges over all possible one- and two-body interactions whereas, in the second sum, σ ranges over all other tensor products of Gell-Mann matrices and the identity. The cost function is

$$F(H) := \sqrt{\sum_{\sigma}^{\prime} h_{\sigma}^2 \sigma + p^2 \sum_{\sigma}^{\prime\prime} h_{\sigma}^2 \sigma}, \quad (71)$$

where p is a penalty paid for applying three- and more-body terms. With the definition of the control cost, it is natural to form a notion of distance in the space $SU(3^n)$ of n -qutrit unitary operators with unit determinant. The function $F(H)$ can be thought of as the norm associated to a (right invariant) Riemannian metric whose metric tensor g has components:

$$g = \begin{cases} 0, & \sigma \neq \tau \\ 1, & \sigma = \tau \text{ and } \sigma \text{ is one or two body} \\ p^2, & \sigma = \tau \text{ and } \sigma \text{ is three or more body} \end{cases}. \quad (72)$$

These components are written with respect to a basis for the local tangent space corresponding to the coefficients h_{σ} . The distance $d(I, U)$ between I and U is defined to be the minimum over all the curves connecting I and U and equal to the minimal length solution to the geodesic equation

$$\left\langle \frac{dH}{dt}, K \right\rangle = i \langle H, [H, K] \rangle, \quad (73)$$

where $\langle \cdot, \cdot \rangle$ denotes the inner product on the tangent space $SU(3^n)$ defined by the metric components (72), and $[\cdot, \cdot]$ denotes the matrix commutator and K is an arbitrary operator in $SU(3^n)$.

All lemmas backing up the final theorem have been proven in detail [4], but the reasoning behind can be summarized in four parts. First let p be the penalty paid for applying three- and more-body items. If one chooses p to be sufficiently large, the distance $d(I, U)$ always has a supremum which is independent of p . Secondly, let $H_P(t)$ be the projected Hamiltonian containing only one- and two-body items, obtained from a Hamiltonian $H(t)$ generating a unitary operator U , and U_P the corresponding unitary operator generated by $H_P(t)$, then

$$\|U - U_P\| \leq 3^n d([U])/p, \quad (74)$$

where $\|\bullet\|$ is the operator norm. Thirdly, if U is an n -qutrit unitary operator generated by $H(t)$ such that $\|H(t)\| \leq c$ in a time interval $[0, \Delta]$, then

$$\|U - \exp(-i\bar{H})\Delta\| \leq 2(e^{c\Delta} - 1 - c\Delta) = O(c^2\Delta^2), \quad (75)$$

where \bar{H} is the mean Hamiltonian. Lastly, for H as an n -qutrit one- and two-body Hamiltonian, a unitary operator U_A exists that satisfies

$$\|e^{iH\Delta} - U_A\| \leq c_2 n^2 \Delta^3 \quad (76)$$

and can be synthesized by using at most $c_1 n^2 / \Delta$ one- and two-qutrit gates, where c_1 and c_2 are constants.

All these lemmas combined gives the final theorem for the qutrit system: for a unitary operator U in $SU(3^n)$, using $O(n^k d(I, U)^3)$ one- and two-qutrit gates is possible to synthesize a unitary U_A satisfying $|U - U_A| \leq c$, where c is any constant. It is worth mentioning that for any family of unitaries U , which is indexed by the number of qudits n , the final theorem shows a quantum circuit exists with a number of gates that is polynomial in $d(I, U)$ and that approximates U to high accuracy. In other words, it is possible to find a polynomial-sized quantum circuit if the distance $d(I, U)$ scales polynomially with n .

With appropriate modification, the Riemannian geometry method can be used to ascertain the circuit-complexity bound for a qudit system [5]. In this scheme, the unitary matrix $U \in SU(d^n)$ is represented by the generalized Gell-Mann matrices as defined in the earlier part of the section. The main theorem in the qudit case is: for any small constant ε , each unitary $U_A \in SU(d^n)$ can be synthesized using $O(\varepsilon^{-2})$ one- and two-qudit gates, with error $|U - U_A| \leq \varepsilon$. To break up the constant ε to an explicit form, we have $\varepsilon^{-2} = N^2 d^4 n^2$, where d is the dimension of the qudit, n is the number of qudits and N is the number of the intervals that $d(I, U)$ divides into, such that a small $\delta = d(I, U)/N \leq \varepsilon$. The qudit case shows the explicit relation between the non-local quantum gate cost and the approximation error for synthesizing quantum qudit operations. In summary, for the quantum circuit model, one can decide a lower bound for the number of gates needed to synthesize U by finding the shortest geodesic curve linking I and U . This provides a good reference for the design of the quantum circuit using qudits.

3 Quantum algorithms using qudits

A qudit, with its multi-dimensional nature, is able to store and process a larger amount of information than a qubit. Some of the algorithms described in this section can be treated as direct generalizations of their qubit counterparts and some utilize the multi-dimensional nature of the qudit at the key subroutine of the process. This section introduces examples of the well-known quantum algorithms based on qudits and divides them into two groups: algorithms for the oracle-decision problems in §3.1 and algorithms for the hidden Abelian subgroup problems in §3.2. Finally, §3.3 discusses how the qudit gates can improve the efficiency of the quantum search algorithm and reduce the difficulty in its physical set-up.

3.1 Qudit oracle-decision algorithm

In this subsection we explore the qudit generalizations of the efficient algorithms for solving the oracle decision problems, which are quite important historically and used to demonstrate the classical-quantum complexity separation [73, 74]. The oracle decision problems are related to the oracle identification problems, which are usually presented in terms of the problem of identifying a unique function f . Simpler than the oracle identification problems, the oracle decision problem is to identify which of the two mutually disjoint sets contains the contents we want. We start in §3.1.1 with a discussion about a single-qudit algorithm that determines the parity of a permutation. In §3.1.2, the Deutsch-Jozsa algorithm in qudit system is discussed and its unique extension, the Bernstein-Vazirani algorithm is provided in §3.1.3.

3.1.1 Parity determining algorithm

In this section we review a single qudit algorithm which provides a two to one speedup than the classical counterpart. This algorithm can also be generalized to work on an arbitrary d -dimensional qudit which solves the same problem of a larger computational space [16]. In quantum computing, superposition, entanglement and discord are known to be the essential parts for the power of quantum algorithms and yet the full picture behind this power is not completely clear [75].

Recent research shows that quantum contextuality is a critical resource for the quantum speedup of a fault tolerant quantum computation mode [76]. The contextual nature can be explained as a particular outcome of a measurement cannot reveal the pre-existing definite value of some underlying hidden variable [77, 78]. In other words, the results of measurements can depend on how we made the measurement, or what combination of measurements we chose to do. For the qudit algorithm discussed below, an unentangled but contextual system can be used to solve a problem faster than classical methods. [16]. Because this qudit algorithm uses a single qudit throughout the process without utilizing any correlation of quantum or classical nature, it acts as a perfect example to study the sources of the quantum speed-up other than the quantum correlation.

The algorithm solves a black-box problems that maps d inputs to d outputs after a permutation. Consider the case of three objects where six possible permutations can be divided into two groups: *even* permutation that is a cyclic change of the elements and *odd* permutation that is an interchange between two elements. If we treat the permutation as a function $f(x)$ that is defined on the set $x \in \{-1, 0, 1\}$, the problems become determining the parity of the bijection $f : -1, 0, 1 \rightarrow -1, 0, 1$. We use Cauchy's two-line notation to define three possible even functions f_k , namely,

$$f_1 := \begin{pmatrix} 1 & 0 & -1 \\ 1 & 0 & -1 \end{pmatrix}, f_2 := \begin{pmatrix} 1 & 0 & -1 \\ 0 & -1 & 1 \end{pmatrix}, f_3 := \begin{pmatrix} 1 & 0 & -1 \\ -1 & 1 & 0 \end{pmatrix}, \quad (77)$$

and the remaining three odd function are

$$f_4 := \begin{pmatrix} 1 & 0 & -1 \\ -1 & 0 & 1 \end{pmatrix}, f_5 := \begin{pmatrix} 1 & 0 & -1 \\ 0 & 1 & -1 \end{pmatrix}, f_6 := \begin{pmatrix} 1 & 0 & -1 \\ 1 & -1 & 0 \end{pmatrix}. \quad (78)$$

The circuit for the single qutrit algorithm in a space spanned by $\{|1\rangle, |0\rangle, |-1\rangle\}$ is shown in Fig. 8, where the operation U_{f_k} applies f_k to the state: $U_{f_k}(|1\rangle + |0\rangle + |-1\rangle) = |f_k(1)\rangle + |f_k(0)\rangle + |f_k(-1)\rangle$, and FT is the single-qutrit Fourier transform

$$FT = \frac{1}{\sqrt{3}} \begin{pmatrix} \omega & 1 & \omega^{-1} \\ 1 & 1 & 1 \\ \omega^{-1} & 1 & \omega \end{pmatrix} \quad (79)$$

using ω as the cube root of unity (14). The process starts with state $|1\rangle$ undergoing FT and becoming $|\psi_1\rangle$ as $FT|1\rangle = |\psi_1\rangle = \omega|1\rangle + |0\rangle + \omega^{-1}|-1\rangle$. Then we obtain $|\psi_k\rangle$ by applying U_{f_k} to $|\psi_1\rangle$. It is easy to show that

$$|\psi_1\rangle = \omega^{-1}|\psi_2\rangle = \omega|\psi_3\rangle \quad (80)$$

and, similarly,

$$|\psi_4\rangle = \omega^{-1}|\psi_5\rangle = \omega|\psi_6\rangle. \quad (81)$$

Hence, application of U_{f_k} on $|\psi_1\rangle$ gives $|\psi_1\rangle$ (up to a phase factor) for an even permutation and $|\psi_4\rangle = FT|-1\rangle$ for an odd permutation. Thus, applying inverse Fourier transform FT^{-1} at the end, we measure $|1\rangle$ for even f_k and $|-1\rangle$ for odd f_k . We are able to determine the parity of f_k by a single application of f_k on a single qutrit.

Moving to a d level quantum system (qudit),

$$|\psi_k\rangle := \frac{1}{\sqrt{d}} \sum_{k'=1}^d \omega^{(k'-1)(k-1)} |k'\rangle. \quad (82)$$

In this scenario, a positive cyclic permutation maps $|\psi_2\rangle$ onto itself whereas negative permutations give $|\psi_d\rangle$. We then measure the results after applying an inverse Fourier transform to solve for the parity of the permutation. This algorithm has been implemented on the NMR system for both the qutrit [15] and ququart [16] cases. It is also realized on a linear optic system [79]. Although the model problem is not one of the most important computational tasks and the speedup is not exponential when generalized to higher dimensional cases, this proposed algorithm provides an elegant yet simple example for quantum computation without entanglement.

3.1.2 Qudit Deutsch-Jozsa algorithm

Deutsch algorithm (with its origin in [73] and improved in [68]) is one of the simplest examples to show the speed advantage of quantum computation. Deutsch-Jozsa algorithm is n -qubits generalization of the Deutsch algorithm. Deutsch-Jozsa algorithm can decide whether a function $f(x)$ is *constant*, with constant

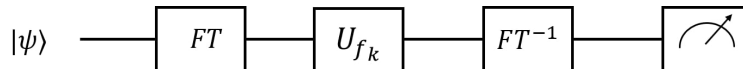


Figure 8: Schematic view of the quantum circuit implementing the parity determining algorithm. FT is the Fourier transform and U_{f_k} is the gate that does one of the two permutations and the last box represents the measurement.

output, or *balanced*, that gives equal instances of both outputs [65]. The process itself consists of only one evaluation of the function $f(x)$. In this algorithm, Alice sends Bob N qubits in the query register and one in the answer register where Bob applies the function to the query register qubits and stores the results in the answer register. Alice can measure the qubits in the query register to determine whether Bob's function is constant or balanced. This algorithm makes use of the superposition property of the qubit and reduces the minimum number of the function call from $2^n/2 + 1$ classically to only 1 with quantum algorithm. This gives another example of the advantages of quantum algorithms.

The Deutsch-Jozsa algorithm can be performed in the qudit system with a similar setup. Furthermore, with the qudit system, Deutsch-Jozsa algorithm can also find the closed expression of an affine function accurate to a constant term [80]. The *constant* and *balanced* function in the n dimensional qudit case have the following definition: An r -qudit multi-valued function of the form

$$f : \{0, 1, \dots, n-1\}^r \rightarrow \{0, 1, \dots, n-1\} \quad (83)$$

is *constant* when $f(x) = f(y) \forall x, y \in \{0, 1, \dots, n-1\}^r$ and is *balanced* when an equal number of the n^r domain values, namely n^{r-1} , is mapped to each of the n elements in the co-domain.

All affine functions

$$f(x_1, \dots, x_r) := A_0 \oplus A_1 x_1 \oplus \dots \oplus A_r x_r, \quad A_0, \dots, A_r \in \mathbb{Z}_n, \quad (84)$$

are either constant or balanced functions of r qudits [80]. If all the coefficients $A_{i \neq 0} = 0$ then the function is constant. For affine function with non-zero coefficient $A_{i \neq 0}$, every element in its domain $\{0, 1, \dots, n-1\}^r$ is reducible modulo n to a unique element $m \in \{0, 1, \dots, n-1\}$, a set of size n . As $f(p) = f(q)$ if $p \equiv q \pmod{n}$, every element in the codomain $\{0, 1, \dots, n-1\}$ is assigned to n^{r-1} different elements in the domain. To finish the proof of the n -ary Deutsch-Jozsa algorithm, another trivial lemma is needed: Primitive n^{th} roots of unity satisfy $\sum_{k=0}^{n-1} \omega^{\alpha k} = 0$ for nonzero integers α .

The circuit of the Deutsch-Jozsa algorithm in qudits is shown in Fig. 9, where the Hadamard gate in the qubit case is replaced with the qudit Fourier transform (reviewed in §3.2.1). This algorithm of r qudits can both distinguish whether a function U_f is balanced or constant and verify a closed expression for an affine function in U_f within a constant term. The constant term is recorded as a universal phase factor of the x -register and thus is lost during

the measurement. The other coefficients of the affine function A_1, \dots, A_r are determined by measuring the state of the x -register at the output, $|A_1, \dots, A_r\rangle$.

A detailed derivation of the circuit has been shown [80], but the reasoning is similar to the qubit version of the Deutsch-Jozsa algorithm. For a constant function U_f the final state after the measurement is $|0\rangle^{\otimes r} |n-1\rangle$ as all basis states in the x -register have null amplitudes for $j \neq 0$. Therefore, if every x -register qudit yields $|0\rangle$, it is a constant function; otherwise the function is balanced.

The Deutsch-Jozsa algorithm in the qudit system shares the same idea while enabling more applications such as determining the closed form of an affine function. Although this algorithm is mainly of theoretical interest, the n -nary version of it may have applications in image processing. It has the potential to distinguish between maps of texture images encoded by affine functions in a Marquand chart with the number of colors corresponding to the size of the radix [23]. This algorithm can also be modified to set up a secure quantum key-distribution protocol [23]. Other proposed Deutsch-Jozsa algorithms exist such as a method that makes use of the artificially allocated subsystems as qudits [81] and a generalized algorithm on the virtual spin representation [82].

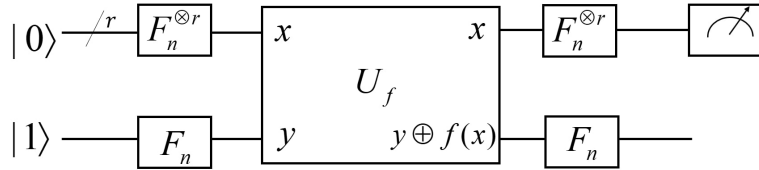


Figure 9: The Deutsch-Jozsa circuit in qudit system. The F_n are the qudit Hadamard gates achieved with quantum Fourier transform.

3.1.3 Qudit generalization of the Bernstein-Vazirani algorithm

in §3.1.2 we have discussed an application of a qudit Deutsch-Jozsa algorithm (DJA): verify a closed expression of an affine function. This application is closely related to the Bernstein-Vazirani algorithm discussed in this section. Given an input string and a function that calculates the bit-wise inner-product of the input string with an unknown string, the Bernstein-Vazirani algorithm determines the unknown string [83]. This algorithm can be treated as an extension of the Deutsch-Jozsa algorithm.

The qudit generalization of the BernsteinVazirani algorithm can determine a number string of integers modulo d encoded in the oracle function [84, 24]. First we introduce a positive integer d and consider the problem in modulo d throughout. Given an N -component natural number string

$$g(a) := (g(a_1), g(a_2), g(a_3), \dots, g(a_N)), \quad g(a_j) \in \{0, 1, \dots, d-1\}, \quad (85)$$

we define

$$f(x) := g(a) \cdot x \pmod{d} = g(a_1)x_1 + g(a_2)x_2 + \dots + g(a_N)x_N \pmod{d}, \quad (86)$$

for

$$x = (x_1, x_2, \dots, x_N) \in \{0, 1, \dots, d-1\}^N. \quad (87)$$

The oracle in the algorithm applies $f(x)$ to the input string x and computes the result, namely, the number string $g(a)$ encoded in the function $f(x)$.

Let us follow the quantum states through the algorithm. The input state x is chosen to be $|\psi_0\rangle = |0\rangle \otimes^N |d-1\rangle$, where $|0\rangle \otimes^N$ means initialization of the N control-qudits into their $|0\rangle$ states and $|d-1\rangle$ means the target qudit is in its $d-1$ state. Quantum Fourier transforms of the pertinent input states are

$$|0\rangle \xrightarrow{QFT} \sum_{y=0}^{d-1} \frac{|y\rangle}{\sqrt{d}} |d-1\rangle \xrightarrow{QFT} \sum_{y=0}^{d-1} \frac{1}{\sqrt{d}} \omega^{d-y} |y\rangle, \quad (88)$$

for ω a root of unity (14). The component-wise Fourier transform of a string encoded in the state $|x_1 x_2 \dots x_N\rangle$ is

$$|x_1 x_2 \dots x_N\rangle \xrightarrow{QFT} \sum_{z \in K} \frac{\omega^{x \cdot z} |z\rangle}{\sqrt{d^N}}, \quad (89)$$

where

$$K = \{0, 1, \dots, d-1\}^N, \quad z := (z_1, z_2, \dots, z_N). \quad (90)$$

We denote the Fourier transform of the $|d-1\rangle$ state as $|\phi\rangle$ and the input state after the Fourier transform is

$$|\psi_1\rangle = \sum_{z \in K} \frac{|x\rangle}{\sqrt{d^N}} |\phi\rangle \quad (91)$$

Now we introduce the oracle as the $O_{f(x)}$ gate such that

$$|x\rangle |j\rangle \xrightarrow{O_{f(x)}} |x\rangle |(f(x) + j) \pmod{d}\rangle, \quad (92)$$

where

$$f(x) = g(a) \cdot x \pmod{d}. \quad (93)$$

By applying the $O_{f(x)}$ gate to $|\psi_1\rangle$ and following the formula by phase kick-back, we obtain the output state

$$O_{f(x)} |\psi_1\rangle = |\psi_2\rangle = \sum_{z \in K} \frac{\omega^{f(x) \cdot z} |x\rangle}{\sqrt{d^N}} |\phi\rangle. \quad (94)$$

Finally, obtain the $|\psi_3\rangle$ which is the state after inverse Fourier transform of the first N qudits of $|\psi_2\rangle$. By measuring the first N quantum state in a d -dimensional space of the state $|\psi_3\rangle$ we can retrieve the following values (as a natural number string offset up to a constant)

$$g(a_1), g(a_2), g(a_3), \dots, g(a_N) \quad (95)$$

using a single query of the oracle function.

The Bernstein-Vazirani algorithm clearly demonstrates the power of quantum computing. The speed of determining the strings has been shown to outperform the best classical case by a factor of N in every cases [84]. The qudit generalizations of the Bernstein-Vazirani algorithm helps us comprehend the potential of the qudit systems.

3.2 Qudit algorithms for the hidden Abelian subgroup problems.

The hidden subgroup problem (HSP) is a topic of research in mathematics and theoretical computer science. Many of the widely used quantum algorithms such as the discrete Fourier transform, the phase estimation and the factoring fit into the framework of this kind of problems. In this section, we review the qudit generalization of these algorithms. The qudit Fourier transform is discussed in §3.2.1 and its application, the PEA is reviewed in §3.2.2. A direct application of these algorithms, the Shor’s factoring algorithm performed with qutrits and in metaplectic quantum architectures is also introduced §3.2.2.

3.2.1 Quantum Fourier Transform with qudits

The quantum Fourier transform algorithm (QFT) is realizable on a qubit system [65]. QFT, as the heart of many quantum algorithms, can also be performed in a qudit system [60, 85]. In an N -dimensional system represented with n d -dimensional qudits, the QFT, $F(d, N)$, where $N = d^n$, transforms the computational basis

$$\{|0\rangle, |1\rangle, \dots, |n-1\rangle\} \tag{96}$$

into a new basis set [25]

$$F(d, N) |j\rangle = \frac{1}{\sqrt{N}} \sum_{k=0}^{N-1} e^{2\pi i j k / N} |k\rangle. \tag{97}$$

For convenience, we write an integer j in a base- d form. If $j > 1$ then

$$j = j_1 j_2 \cdots j_n = j_1 d^{n-1} + j_2 d^{n-2} + \cdots + j_n d^0 \tag{98}$$

and, if $j < 1$, then

$$j = 0.j_1 j_2 \cdots j_n = j_1 d^{-1} + j_2 d^{-2} + \cdots + j_n d^{-n}. \tag{99}$$

The QFT acting on a state $|j\rangle$ can be derived and rewritten in a product form as

$$\begin{aligned}
|j\rangle = |j_1 j_2 \cdots j_n\rangle &\mapsto \frac{1}{d^{n/2}} \sum_{k=0}^{d^n-1} e^{2\pi i j k / d^n} |k\rangle \\
&= \frac{1}{d^{n/2}} \sum_{k_1=0}^{d-1} \cdots \sum_{k_n=0}^{d-1} e^{2\pi i j (\sum_{l=1}^n k_l d^{-l})} |k_1 k_2 \cdots k_n\rangle \\
&= \frac{1}{d^{n/2}} \sum_{k_1=0}^{d-1} \cdots \sum_{k_n=0}^{d-1} \bigotimes_{l=1}^n e^{2\pi i j k_l d^{-l}} |k_l\rangle \\
&= \frac{1}{d^{n/2}} \bigotimes_{l=1}^n \left[\sum_{k_l=0}^{d-1} e^{2\pi i j k_l d^{-l}} |k_l\rangle \right].
\end{aligned}$$

This process can be realized with the quantum circuit shown in Fig. 10, and the fully expanded expression of the product form is shown on the right side of the figure. The generalized Hadamard gate H^d in the figure is defined as $H^d := F(d, d)$ which effects the transform

$$H^d |j_n\rangle = |0\rangle + e^{2\pi i 0 \cdot j_n} |1\rangle + \cdots + e^{2(d-1)\pi i 0 \cdot j_n} |d-1\rangle. \quad (100)$$

The matrix representation of H^d is

$$\begin{pmatrix}
1 & 1 & \cdots & 1 \\
1 & e^{2\pi i 0 \cdot 1} & \cdots & e^{2\pi i 0 \cdot (d-1)} \\
\vdots & \vdots & \ddots & \vdots \\
1 & e^{2(d-1)\pi i 0 \cdot 1} & \cdots & e^{2(d-1)\pi i 0 \cdot (d-1)}
\end{pmatrix}. \quad (101)$$

In the circuit the R_k^d gate is a phase gate that has the expression

$$R_k^d = \begin{pmatrix}
1 & 0 & \cdots & 0 \\
0 & e^{2\pi i / d^k} & \cdots & 0 \\
\vdots & \vdots & \ddots & \vdots \\
0 & 0 & \cdots & e^{2\pi i (d-1) / d^k}
\end{pmatrix}. \quad (102)$$

The black dots in the circuit are multi-value-controlled gates that apply R_k^d to the target qudit j times for a control qudit in state $|j\rangle$. A straightforward derivation shows that the circuit produces the results on the left side of the figure. In order to complete the Fourier transform and ensure the correct sequence of $j_1 j_2 \cdots j_n$, a series of SWAP gates are applied at the end, which are not explicitly drawn in Fig. 10.

The QFT developed in qudit system offers a crucial subroutine for many quantum algorithm using qudits. Qudit QFT not only offers superior approximations where the error magnitude (caused by eliminating controlled phase shift gates that implement very small rotations) decreases exponentially with d but also achieves smaller error bounds [85], which outperforms the binary case [86].

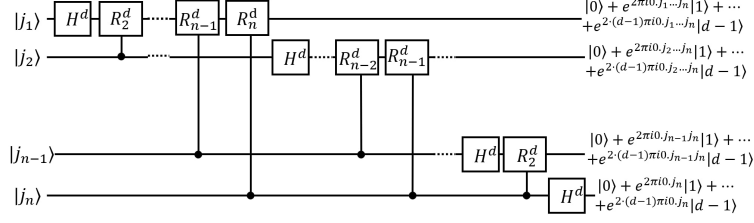


Figure 10: Quantum Fourier transform in qudit system. H^d is the d -dimensional Hadamard gate and the expression of the R^d gate is shown in Eq. (102). Resultant states are shown to the right.

3.2.2 Phase-estimation algorithm with qudits

With the qudit quantum Fourier transform, we are able to generalize the PEA to qudit circuits [25]. Similar to the PEA using qubit, the PEA in the qudit system is composed by two registers of qudits. The first register contains t qudits and t depends on the accuracy we want for the estimation. We assume that we can perform a unitary operation U to an arbitrary number of times using qudit gates and generate its eigenvector $|u\rangle$ and store it using the second register's qudits [26]. We want to calculate the eigenvalue of $|u\rangle$ where $U|u\rangle = e^{2\pi i r} |u\rangle$ by estimating the phase factor r .

For convenience, we rewrite the rational number r as

$$r = R/d^t = \sum_{l=1}^t \bar{R}_l/d^l = 0.\bar{R}_1\bar{R}_2 \dots \bar{R}_t. \quad (103)$$

As shown in Fig. 11, each qudit in the first register passes through the generalized Hadamard gate $H \equiv F(d, d)$. For the l^{th} qudit of the first register, we have

$$F(d, d) |0\rangle_l = \frac{1}{\sqrt{d}} \sum_{k_l=0}^{d-1} |k_l\rangle. \quad (104)$$

Then the l^{th} qudit is used to control the operation $U^{d^{t-l}}$ on the target qudits of the state $|u\rangle$ in the second register, which gives

$$CU^{d^{t-1}} |k\rangle \otimes |u\rangle = |k\rangle (U^{d^{t-1}})^k |u\rangle = e^{2\pi i k d^{t-1} r} |k\rangle \otimes |u\rangle. \quad (105)$$

Note that the function of the controlled operation $CU^{d^{t-1}}$ can be considered as a 'quantum multiplexer' [32, 87, 70]. After executing all the controlled operations on the qudits, the qudit system state turns out to be

$$\left(\prod_{l=1}^t \otimes \frac{1}{\sqrt{d}} \sum_{k_l=0}^{d-1} e^{2\pi i k_l d^{t-l} r} |k_l\rangle \right) \otimes |u\rangle. \quad (106)$$

Therefore, through a process called the “phase kick-back”, the state of the first register receives the phase factor and becomes

$$|\text{Register 1}\rangle = \frac{1}{d^{t/2}} \sum_{k=0}^{d^t-1} e^{2\pi i r k} |k\rangle. \quad (107)$$

The eigenvalue r which is represented by the state $|R\rangle$ can be derived by applying the inverse QFT to the qudits in the first register:

$$F^{-1}(d, d^t) |\text{Register 1}\rangle = |R\rangle. \quad (108)$$

The whole process of PEA is shown in Fig. 12. To obtain the phase $r = R/d^t$ exactly, we can measure the state of the first register in the computational basis.

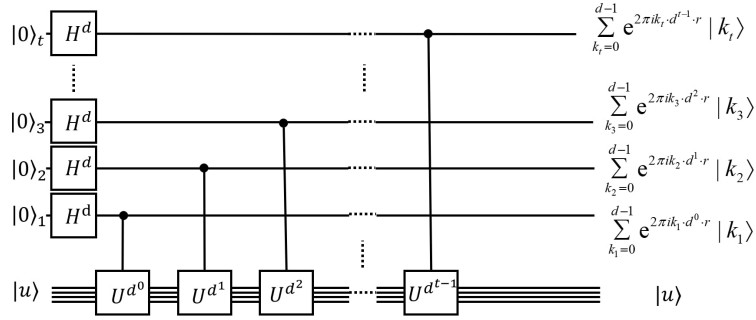


Figure 11: The circuit for the first stage of the PEA. The qudits in the second register whose states represent $|u\rangle$ are undergoing the U operations and the generated phase factors are kicking back to the qudits in the first register, giving the results to the right.

The PEA in qudit system provides a dramatic improvement in the number of qudits required when compared to the binary case and the error rate decreases exponentially as the qudit dimension increases [88]. A long list of PEA applications includes the Shor’s factoring algorithm [67], simulation of quantum systems [89], solving linear equations [90, 91], and quantum counting [92]. To give some examples, a quantum computer simulator which uses the PEA algorithm has been used to calculate the molecular ground-state energies [66] and to obtain the energy spectra of molecular systems [93, 94, 95, 96, 97, 98]. Recently, a method to solve the linear system using a qutrit version of the PEA has been proposed [99]. The qudit version of the PEA opens the possibility to realize all those applications that have the potential to out-perform their qubit counterparts.

The Shor’s quantum algorithm for integer factorization serves as a striking example of super-polynomial speed-up offered by a quantum algorithm over the best-known classical algorithms [100]. The order-finding algorithm at the core

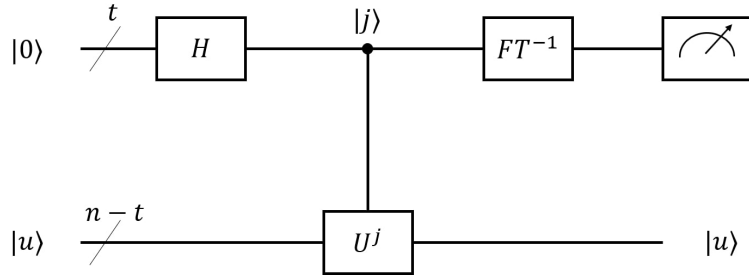


Figure 12: The schematic circuit for the whole stage of PEA. After the first stage of the PEA, inverse Fourier transform(FT^{-1}) is applied to the qudits in the first register and the phase factors can be obtained by measuring the states of the first register qudits.

of the factoring algorithm is a direct application of the PEA. With the previous discussion on the qudit versions of the quantum Fourier transform and phase estimation, we have the foundation to generalize the Shor’s factoring algorithm to the higher dimensional qudit system. Several proposals for performing the Shor’s algorithm on the qudit system, such as the implementation of an adiabatic quantum algorithm for factorization on two qudits with the number of levels d_1 and d_2 [6], exist. This method makes use of a time-dependent effective Hamiltonian in the form of a sequence of rotation operators that are selective with respect to the transitions between neighboring levels of a qudit.

Another proposal carries out a comparative resource cost analysis targeting two prospective quantum ternary platforms [26]. One is the “generic” platform that uses magic state distillation for universality [52]. The other, known as a metaplectic topological quantum computer (MTQC), is a non-Abelian anyonic platform, where universality is achieved by a relatively inexpensive protocol based on anyonic braiding and interferomic measurement [8, 9]. The article discusses two different logical solutions for the modular exponential circuit of the Shor’s period-finding function on each of the two platforms: one that encodes the integers with the binary subspace of the ternary state space and employs the ternary optimizations of known binary arithmetic circuits; the other encodes the integer directly in the ternary space using the arithmetic circuits stemming in Ref [10]. Significant advantages for the MTQC platform are found compared to other platforms. In particular the MTQC platform allows factorization of an n -bit number using the smallest possible number of $n + 7$ logical qutrits at the cost of inflating the depth of the logical circuit by a logarithmic factor. To sum up the comparison, the MTQC provides significant flexibility at choosing period finding solutions for ternary quantum computers of varying sizes.

3.3 Quantum search algorithm with qudits

The quantum search algorithm, also known as the Grover's algorithm, is one of the most important quantum algorithms that illustrates the advantage of quantum computing. The Grover's algorithm is able to outperform the classical search algorithm for a large database. The size of the computational space in an n -qubit system is a Hilbert space of 2^n dimensions.

As practical limitations for increasing the number of qubits exist, the working Hilbert space can be expanded by increasing the dimension of each carrier of information, i.e., using qudits and qudit gates. Several schemes of Grover's quantum search with qudits have been proposed, where the Hadamard gate in the qubit system is replaced by a discrete Fourier transform [101] or another d -dimensional transformation [102] for the construction of the reflection-about-average operator (also known as the diffusion operator). In this section, an instruction on setting up the Grover's algorithm in the qudit system is reviewed as well as a proposal of a new way to build a quantum gate F that drives the single qudit state into an equal-weight superposition state [27]. With the new gate F , it is easier to realize the Grover's algorithm in a physical system and improve the overall efficiency of the circuit.

The Grover's algorithm solves the unstructured search problem by applying the Grover's oracle iteratively. To construct the oracle, we build qudit gates to perform the oracle function $f(x)$ that acts differently on one marked element s as compared to all the others. The logic behind the algorithm is to amplify the amplitude of the marked state $|s\rangle$ with the oracle function, while attenuating the amplitudes of all the other states. The marked state is amplified enough to be located in $O(\sqrt{N})$ steps for an N dimensional search space. In each step the Grover's oracle is executed one time. This oracle can be broken into two parts: (1) *Oracle query*: the oracle shifts the phase of the marked state $|s\rangle$ and leaving others unchanged by doing

$$\mathbf{R}_s(\phi_s) = \mathbf{1} + (e^{i\phi_s} - 1) |s\rangle \langle s|. \quad (109)$$

(2) *Reflection-about-average*. This operation is a reflection about a vector $|a\rangle$ with a phase ϕ_a :

$$\mathbf{R}_a(\phi_a) = \mathbf{1} + (e^{i\phi_a} - 1) |a\rangle \langle a|. \quad (110)$$

It is constructed by applying the generalized Hadamard gate H , applying phase shift to $|0\rangle$ state and then applying H again. It is straightforward to show that

$$H^{\otimes n} \mathbf{R}_0(\phi_0) H^{\otimes n} = \mathbf{R}_a(\phi_a).$$

The two steps combined form the Grover's operator \mathbf{G} , which is one execute of the Grover's iteration.

Building Grover's operator in a qudit system can be simplified both algorithmically and physically. The most important improvement can be achieved by replacing the Hadamard gate H with F which drives the single-qudit state

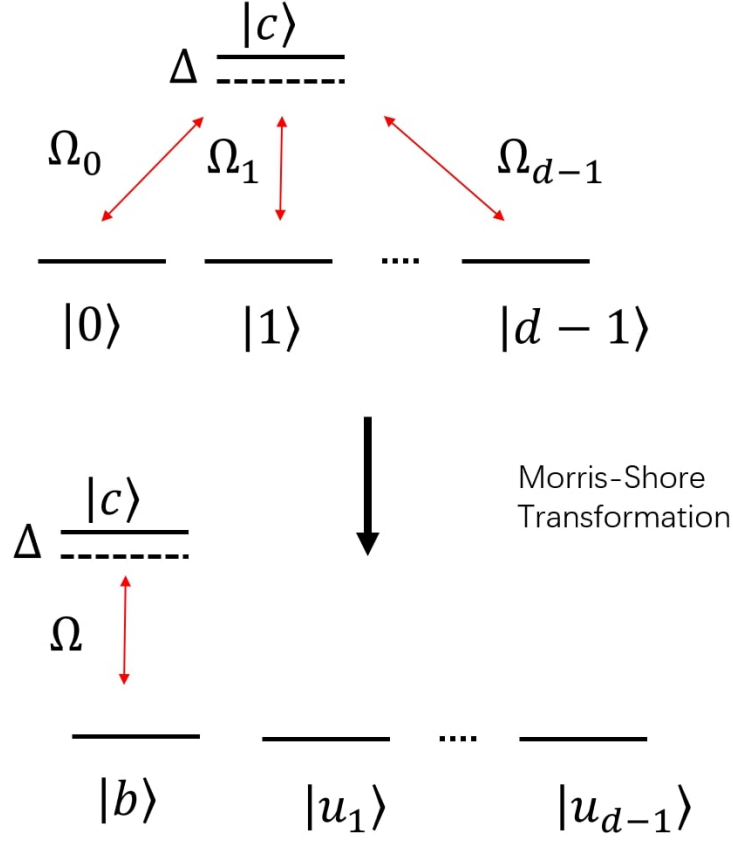


Figure 13: Qudit in a multipod linkage: linkage patterns in the original basis (top) and in the Morris-Shore basis (bottom). The qudit is formed of states $|0\rangle, |1\rangle, \dots, |d-1\rangle$, which are coupled to each other by two-photon Raman processes via a common (ancilla) state $|c\rangle$ with a common detuning Δ , but different single-photon Rabi frequencies Ω_k . The multipod in the Morris-Shore basis reduces to a two-state quantum system formed of a bright state $|b\rangle$ and the original ancilla state $|c\rangle$, coupled by the (rms) Rabi frequency Ω . State $|b\rangle$ is a superposition of the qudit states weighted by the couplings Ω_k ; $|u_n\rangle$ are uncoupled (dark) states, which do not participate in the dynamics.

$|0_k\rangle$ into an equal weight superposition state,

$$F|0_k\rangle = \sum_{q=0}^{d-1} \xi_q |q_k\rangle, \quad (111)$$

with $|\xi_q| = d^{-1/2}$, in all qudits ($k \in \{1, 2, \dots, n\}$). The proposed F gate is

achieved in a single physical interaction, which does not even assume any phase relations between the fields driving individual qudits. The F can be constructed relatively easily in a multipod system, which is a system of d degenerate quantum states $|0\rangle, |1\rangle, \dots, |d-1\rangle$, coupled to each other by two-photon Raman processes via a common (ancilla) state $|c\rangle$, as illustrated in Fig. 13.

We assume hereafter that all coupling fields coincide in time and the dynamics of the multipod system is reducible by the Morris-Shore transformation [103] to a two state system illustrated in the bottom of Fig. 13. The two states are coupled by the root-mean-square (rms) Rabi frequency

$$\Omega(t) = \sqrt{\sum_{k=0}^{d-1} |\Omega_k(t)|^2}. \quad (112)$$

Then the dynamics of the multipod can be derived from the two-state solution [104]. The propagator for the qudit manifold for rms pulse area

$$A = \Omega \int_{-\infty}^{\infty} dt f(t) \quad (113)$$

is the generalized reflection $\mathbf{R}_\chi(\phi)$ with

$$|\chi\rangle = \frac{1}{\Omega} (\Omega_0, \Omega_1, \dots, \Omega_{d-1})^T. \quad (114)$$

The acquired phase ϕ depends on the pulse shape $f(t)$ and the detuning.

This method of building F minimizes the number and the duration of algorithmic steps and thus is fast to implement and, in addition, it also provides better protection against detrimental effects such as decoherence or imperfections. Due to its conceptual simplicity, this method has applications in numerous physical systems. Thus, it is one of the most natural and simplest realizations of Grover's algorithm in qudits.

4 Implementations of qudits

The qubit circuit and qubit algorithm have been implemented on various physical systems such as defects in solids [105, 106, 107], quantum dots [108, 109], photons [110, 111], super conducting systems [112, 113], trapped ions [114, 115], magnetic [116, 117, 118, 119] and non-magnetic molecules [120, 121]. For each physical representation of the qubit, only two levels of states are used to store and process quantum information. However, many quantum properties of these physical systems have more than two levels, such as the frequency of the photon [2], energy levels of the trapped ions [14], spin states of the nuclear magnetic resonance systems [15] and the spin state of the molecular magnetic magnets [122]. Therefore, these systems have the potential to represent qudit systems. In this section, we briefly review several physical platforms that have been used to implement qudit gates or qudit algorithms.

Although most of the systems have three or four levels available for computation, they are extensible to higher level systems and scalable to multi-qudit interactions. These pioneer implementations of qudit systems show the potential of future realization of the more powerful qudit quantum computers that have real-life applications.

4.1 Time and frequency bin of a photon

Photonic system is a good candidate for quantum computing because photons rarely interact with other particles and thus have a comparatively long decoherence time. In addition, photon has many quantum properties such as the orbital angular momentum [123, 124], frequency-bin [125, 126, 127, 128] and time-bin [129, 130] that can be used to represent a qudit. Each of these properties provides an extra degree of freedom for the manipulation and computation. Each degree of freedom usually has dimensions greater than two and thus can be used as a unique qudit. The experimental realization of arbitrary multidimensional multiphotonic transformations has been proposed with the help of ancilla state, which is made possible by the introduction of a new quantum nondemolition measurement and the exploitation of a genuine high-dimensional interferometer [11]. Experimental entanglement of high-dimensional qudits, where the photons are created in a coherent superposition of multiple high-purity frequency modes is also developed and demonstrated. [125].

Here we review a single photon system that has demonstrated a proof-of-principle qutrit PEA [2]. In a photonic system, there is no deterministic way to interact two photons and thus it is hard to build a reliable controlled gate for the photonic qudits. The following photonic system bypasses this difficulty via using the two degrees of freedom on a single photon—i.e., the time-bin and frequency-bin to be the two qutrits. The frequency degree of freedom carries one qutrit as the control register and the time degree of freedom carries another qutrit as the target register. The experimental apparatus consists of the well-established techniques and fiber-optic components: continuous-wave(CW) laser source, phase modulator(PM), pulse shaper(PS), intensity modulator(IM) driven by an arbitrary waveform generator and chirped fiber Bragg grating(CFBG).

The device is divided into three parts [2]: 1. A state preparation part that comprises a PM followed by a PS and a IM that encodes the initial state to qudits; 2. a controlled-gate part that is built with a PM sandwiched by two CFBGs to perform the control- U operation; and 3. an inverse Fourier transformation comprising a PM and then a PS to extract the phase information. Note that the controlled-gate part can perform a multi-value-controlled gate that applies different operations based on the three unique states of the control qutrit.

In the PEA procedure, eigenphases representable by one ternary digit (given by a single controlled qutrit) are retrieved with 98% fidelity. In addition to having long coherence lifetime, the photonic system also has a unique advantage over other common quantum devices i.e., the ability to process and measure thousands of photons simultaneously. This allows us to generate statistical

patterns quickly and infer the phase accurately whereas the normal PEA has to use additional qudits on the control register to increase accuracy.

\hat{U}_1			
Eigenstate	$ 0\rangle_t$	$ 1\rangle_t$	$ 2\rangle_t$
E_0	$.9948 \pm .0004$	$.0101 \pm .0004$	$.0122 \pm .0005$
E_1	$.0023 \pm .0002$	$.9805 \pm .0009$	$.0120 \pm .0005$
E_2	$.0029 \pm .0002$	$.0094 \pm .0004$	$.9758 \pm .0010$
True Phase, ϕ	0	$2\pi/3$	$4\pi/3$
Est. Phase, $\check{\phi}$	1.972π	$.612\pi$	1.394π
Error, $\frac{ \phi-\check{\phi} }{2\pi}$	1.4%	2.7%	3.0%
\hat{U}_2			
Eigenstate	$ 0\rangle_t$	$ 1\rangle_t$	$ 2\rangle_t$
E_0	$.878 \pm .002$	$.316 \pm .003$	$.143 \pm .002$
E_1	$.032 \pm .001$	$.530 \pm .003$	$.318 \pm .003$
E_2	$.090 \pm .002$	$.154 \pm .002$	$.539 \pm .003$
True Phase, ϕ	0	$.3511\pi$	1.045π
Est. Phase, $\check{\phi}$	1.859π	$.377\pi$	1.045π
Error, $\frac{ \phi-\check{\phi} }{2\pi}$	7.1%	1.3%	0.0%

Table 1: Normalized photon counts and comparison of the true phase ϕ and the experimentally estimated phase $\check{\phi}$ for each eigenstate of \hat{U}_1 (Eq. 115) and \hat{U}_2 (Eq. 116).

Here we provide an example for the statistical inference of the phase based on numerical data generated by the photonic PEA experiment just described. The two unitary operations used in the experimental setup are

$$\hat{U}_1 = \text{diag}(1, \omega, \omega^2), \quad (115)$$

with ω being the cube root of unity (14), and

$$\hat{U}_2 = \text{diag}(1, e^{i0.351\pi}, e^{i1.045\pi}). \quad (116)$$

In the experiment, photonic qutrits are sent through the control and target registers and the state of the control register qutrits is measured and counted to obtain the phase information.

When the input target register of a PEA circuit is an eigenstate with a corresponding eigenphase ϕ , the probability for the qutrit output control state to collapse to $|n\rangle$, where $n \in \{0, 1, 2\}$, is

$$C(n, \phi) = \frac{1}{9} \left| 1 + e^{i(\phi - \frac{n2\pi}{3})} + e^{i2(\phi - \frac{n2\pi}{3})} \right|^2. \quad (117)$$

Now let E_0 , E_1 , and E_2 be the measured, normalized ($\sum E_n = 1$) photon counts projected, respectively, onto $|0\rangle_f$, $|1\rangle_f$, and $|2\rangle_f$. The phase we estimate from

our measurement, denoted $\tilde{\phi}$, is the phase that minimizes the mean-square error between the measured and theoretical probabilities:

$$\min_{\tilde{\phi}} \sum_{n=0}^2 (E_n - C(n, \tilde{\phi}))^2 \quad (118)$$

The estimated phases for \hat{U}_1 (115) and \hat{U}_2 (116) are shown in Table 1 [2]. The first experiment with U_1 estimates the phase of an eigenvector and gives the eigenvalue. The second experiment with U_2 estimates the phase of a state with an arbitrary value (not a fraction of π), but, by repeating the experiment, the eigenvalue can be estimated from the statistical distribution of the results.

4.2 Ion trap

Intrinsic spin, an exclusively quantum property, has an inherently finite discrete state space which is a perfect choice for representing qubit or qudit. When a charged particle has spin, it possesses a magnetic momentum and is controllable by external electromagnetic pulses. This concept leads to the idea of ion trap where a set of charged ions are confined by electromagnetic field. The hyperfine (nuclear spin) state of an atom, and lowest level vibrational modes (phonons) of the trapped atoms serve as good representations of the qudits. The individual state of an atom is manipulated with laser pulse and the ions interact with each other via a shared phonon state.

The set-up of an ion trap qutrit system reviewed here can perform arbitrary single qutrit gates and a control-not gate [14]. These two kinds of gates form a universal set and thus can be combined to perform various quantum algorithms such as those discussed in §3. The electronic levels of an ion are shown in Fig. 14. The energy levels $|0\rangle, |1\rangle, |2\rangle$ are used to store the quantum information of a qutrit. The $|0'\rangle$ is an auxiliary level necessary when defining the conditional two-qutrit gate. The transition between the levels are driven by the classical fields $\Omega_{03}, \Omega_{13}, \Omega_{04}$ and Ω_{24} of the Raman transitions through independent channels linked to orthogonal polarizations. In the case of single qutrit gates, where the center-of-mass motion is excluded, and assuming the conditions

$$\Delta = (\omega_4 - \omega_0) - \nu_2 = (\omega_3 - \omega_0) - \nu_2 = (\omega_4 - \omega_2) - \nu_1 = (\omega_3 - \omega_1) - \nu_1 \quad (119)$$

and

$$\Delta \gg \Omega_{04}, \Omega_{03}, \Omega_{31}, \Omega_{42}, \quad (120)$$

the effective Hamiltonian describing the ion is

$$\frac{H}{\hbar} = -\frac{|\Omega_{31}|^2}{\Delta} |1\rangle \langle 1| - \frac{|\Omega_{42}|^2}{\Delta} |2\rangle \langle 2| - \frac{|\Omega_{30}|^2 + |\Omega_{40}|^2}{\Delta} |0\rangle \langle 0| - \quad (121)$$

$$- \left[\frac{\Omega_{31}\Omega_{30}^*}{\Delta} |0\rangle \langle 1| + \frac{\Omega_{42}\Omega_{40}^*}{\Delta} |0\rangle \langle 2| + \text{hc} \right]. \quad (122)$$

The evolution operator in the restricted three-dimensional space spanned by $\{|2\rangle, |1\rangle, |0\rangle\}$ is

$$U(\varphi) = \begin{pmatrix} 1 + |g|^2 C(\varphi) & gg'^* C(\varphi) & -ig \sin \varphi \\ g'g^* C(\varphi) & 1 + |g'|^2 C(\varphi) & -ig' \sin \varphi \\ -ig^* \sin \varphi & -ig'^* \sin \varphi & \cos \varphi \end{pmatrix}, \quad (123)$$

where $\varphi = \Omega t$ represents interaction time and

$$C(\varphi) = \cos \varphi - 1, \quad \Omega^2 = |\kappa'|^2 + |\kappa|^2. \quad (124)$$

The notation g and g' represents

$$g := \kappa/\Omega, \quad g' = \kappa'/\Omega, \quad \kappa := \Omega_{42}^* \Omega_{40}/\Delta, \quad \kappa' = \Omega_{31}^* \Omega_{30}/\Delta. \quad (125)$$

All kinds of transitions can be addressed by manipulating the κ and κ' coupling.

The conditional two-qutrit gate is achievable via the center-of-mass (CM) motion of ions inside the trap which is addressed by adjusting a Raman transition to a given red sideband. The ion CM coupled to the electronic transition $|0\rangle \rightarrow |q\rangle$ is described by the Hamiltonian

$$H_{n,q} = \frac{\Omega_q \eta}{2} [|q\rangle_n \langle 0| a e^{-i\delta t - i\phi} + a^\dagger |0\rangle_n \langle q| e^{i\delta t + i\phi}]. \quad (126)$$

Here a and a^\dagger are the annihilation and creation operators of the CM phonons, respectively, and Ω_q is the effective Rabi frequency after adiabatic elimination of upper excited levels, ϕ is the laser phase, and

$$\delta = \omega_2 - \omega_0 - \nu_2 + \nu_1 + \nu_x = \omega_1 - \omega_0 - \nu_2 + \nu_1 + \nu_x \quad (127)$$

is the detuning. The Lamb-Dicke parameter is

$$\eta := \sqrt{\hbar k_\theta^2 / (2M\nu_x)}. \quad (128)$$

With appropriate selection of effective interaction time and laser polarizations, the CM motion coupled to electronic transitions is coherently manipulated. This Hamiltonian governs coherent interaction between qutrits and collective CM motion.

To complete the universal quantum computation requirements, a measurement scheme in the computational basis is needed. In this scheme, von Neumann measurements distinguishing three directions $|0\rangle$, $|1\rangle$, $|2\rangle$ are accomplished by connecting resonant interactions from $|1\rangle$ and $|2\rangle$ to states $|3\rangle$ and $|4\rangle$, respectively. The single and two-qutrit controlled gate are combined to perform various qutrit algorithms such as the quantum Fourier transform. Other variations of the ion-trap qutrit quantum computer designs use trapped ions in the presence of a magnetic field gradient [131]. The qutrit ion-trap computer provides a significant increase of the available Hilbert space while demanding only the same amount of physical resources.

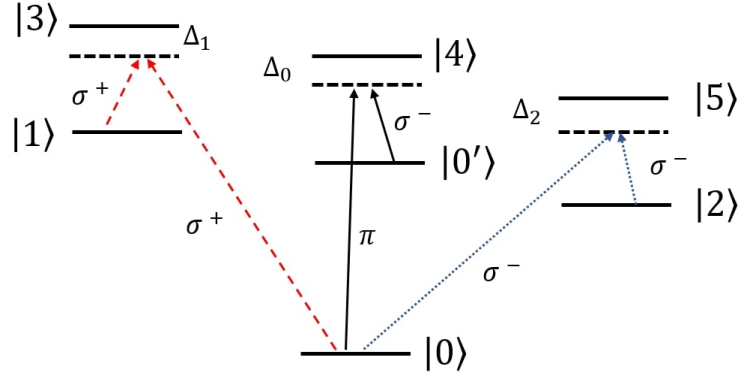


Figure 14: Electronic level structure of the trapped ion. Quantum information of the qutrit is stored in levels $|0\rangle$, $|1\rangle$, and $|2\rangle$. The transitions involving effective interactions between levels $|0\rangle \rightarrow |1\rangle$ and $|0\rangle \rightarrow |2\rangle$ are driven by classical fields with different polarizations.

4.3 Nuclear magnetic resonance

Nuclear magnetic resonance (NMR) is widely used in chemistry and involves manipulating and detecting molecules' nuclear spin states using radio-frequency electromagnetic waves [132]. Some technologies of this field are sophisticated enough to control and observe thousands of nuclei in an experiment. The NMR has the potential to scale up quantum computer to thousands of qudits [133]. Some features of an NMR system for quantum computing include techniques for controlling realistic Hamiltonians to perform arbitrary unitary transforms, methods for characterizing and circumventing decoherence, and considerations which arise in assembling components in implementing full quantum algorithms on entire systems [65].

In this section we review the implementation of a single-qudit algorithm that can determine the parity of a permutation on an NMR system [15]. The algorithm itself is the parity determining algorithm explained in §3.1.1. The experiment uses a deuterated chloroform molecule oriented in a lyotropic liquid crystal as the NMR system and the deuterium nucleus serves as a single qutrit. The lyotropic liquid crystal is composed of 25.6% of potassium laurate, 68.16% of H₂O and 6.24% of decanol, and 50 μ l of Chloroform-D is added to 500 μ l of liquid crystal. The molecule is embedded in a liquid crystalline environment and the anisotropic molecular orientation with respect to the strong magnetic field. This gives rise to a finite quadrupolar coupling term in the Hamiltonian given by

$$H = -\omega_0 I_z + \Lambda(3I_z^2 - I^2), \quad (129)$$

where $\Lambda = e^2 q Q S / 4$ is the effective value of the quadrupolar coupling.

All such experiments have been performed at 277 K on a 600 MHz Avance III NMR spectrometer equipped with a QXI probe, with the deuterium nucleus resonating at 91.108 MHz. The deuterium relaxation times T_1 and T_2 were of the order of 170 ms and 50 ms respectively. The Fourier transformation is implemented by a sequence of three transition-selective pulses, namely,

$$(270)_{x23}(109.47)_{y12}(90)_{y23}. \quad (130)$$

Permutations are implemented by various combinations of 180° transition-selective as well as non-selective pulses.

Final states of the system can be distinguished by a single projective measurement. True projective measurements are not possible on an ensemble NMR quantum computer, although their effect has been approximated using pseudopure spin states [134]. To compute resemblance of the experimental and theoretical density matrices, the fidelity measure

$$F := \frac{\text{tr}(\rho_{\text{th}}^\dagger \rho_{\text{expt}})}{\sqrt{\text{tr}(\rho_{\text{th}}^\dagger \rho_{\text{th}})} \sqrt{\text{tr}(\rho_{\text{expt}}^\dagger \rho_{\text{expt}})}} \quad (131)$$

is used, where ρ_{th} and ρ_{expt} are, respectively, theoretically expected and experimentally obtained density matrices. Fidelities obtained for these proposed operations are 0.92 and above.

Another set-up of the same algorithm treats a single ququart [16]. The algorithm implementation is achieved using a spin $\frac{3}{2}$ nuclei, which has been extensively used in NMR-QIP applications. In their NMR systems, a strong static magnetic field is responsible for the Zeeman splitting, providing four energy levels. All of the two implementations of the single-qudit algorithm show that the NMR system provides a way to realize a reliable and efficient qudit system for the quantum computing.

4.4 Molecular magnets

Molecular quantum magnets, also called the single-molecule magnets (SMM), provides another physical representation of qudits [122]. They have phenomenal magnetic characteristics and can be manipulated via chemical means. This allows the modification of the ligand field of the spin carriers as well as the interaction between the SMM with the other units. In one out of several schemes, the nuclear spin states of the molecules, which have a long life-time, are used to store the quantum information, while their electronic states are used to read-out the quantum information. In the mean time, the molecule is extremely robust, allowing its deposition in a number of substrates at high temperatures conserving its molecular, electronic and magnetic characteristics [135].

As one of the SMMs, the single molecule TbPc₂ complex reviewed in this section possesses all necessary properties such as long lifetime and robustness. These properties are integrated as active units into a serious quantum mechanical devices such as molecular spin valve [136], resonator [137] and

transistor [99, 138]. The SMM properties of TbPc₂ can be attributed to the strong spinorbit coupling of lanthanide ions and the ligand field exerted by the phthalocyanines, yielding a highly axial ground state characterised by an $|J = 6, J_z = \pm 6\rangle$ of the ⁷F₆ manifold [139]. Magnetic properties of TbPc₂ are governed by the Hamiltonian:

$$\mathcal{H} = \mathcal{H}_{lf} + g_J \mu_0 \mu_B J \cdot H + A_{hf} I \cdot J + (I_z^2 - \frac{1}{3}(I+1)I), \quad (132)$$

where \mathcal{H}_{lf} is the ligand field Hamiltonian, and the second term represents the Zeeman energy. The third term accounts for hyperfine interactions and the fourth term is the quadrupole term. A sweeping magnetic field associated with $m_I = \pm 1/2$ and $\pm 3/2$ can cause quantum tunnelling of magnetisation, which preserves nuclear spin while changing electronic magnetic moment. This field enables nuclear-spin measurement by suspending the TbPc₂ molecule on carbon nanotubes (CNT) and between gold junctions.

This measurement uses the technique of electro-migration. Initialisation and manipulation of the four spin states of TbPc₂ can be obtained from QTM transitions driven by external ramping magnetic field between ± 60 mT, while monitoring the conductance jump of the readout dot. The transitions between the $|+1/2\rangle \leftrightarrow |-1/2\rangle$ states and $|+3/2\rangle \leftrightarrow |-3/2\rangle$ is achieved via applying appropriate resonate frequencies ν_{12} and ν_{23} . Relaxation and coherence times are important aspects to be analyzed for the TbPc₂ system, and this process is accomplished by the real-time imaging of the nuclear spin trajectory recorded after initialisation.

Statistical analysis of the nuclear spin coherence time makes use of the spinlattice relaxation times by fitting the data for an exponential form ($y = \exp(-t/T_1)$) and yields $T_1 \approx 17$ s for $m_I = \pm 1/2$ and $T_1 \approx 34$ s for $m_I = \pm 3/2$ with fidelities of $F(m_I = \pm 1/2) \approx 93\%$ and $F(m_I = \pm 3/2) \approx 87\%$ accordingly. The TbPc₂ SMM can be used to execute Grover's algorithm, where the manipulation of each individual m_I state contained in the TbPc₂ molecular qubit are addressed via resonance frequencies [17, 140].

To realize the Grover's algorithm, simultaneous manipulation of m_I states is achieved, allowing the creation superposition of the four nuclear spin states, embedded in the qudit (with $d = 4$ for $I = 3/2$). In summary, this review shows that the molecular multilevel nuclear spin qubits meet practically all the essential characteristics to perform quantum operations [141], which are: (i) isolation, (ii) initialisation, (iii) read out, (iv) long coherence times and (v) manipulation, ultimately leading to the realisation of the Grovers algorithm.

5 Summary and future outlook of qudit system

This review article introduces the basics of the high-dimensional qudit systems and provides details about qudit gates, qudit algorithms and implementations on various physical systems. The article serves as a summary of recent developments of qudit quantum computing and an introduction for newcomers to the

field of qudit quantum computing. Furthermore we show the advantages and the potential for qudit systems to outperform qubit counterparts.

Qubit algorithms can be generalized and performed with qudits. We have discussed topics concerning qudit gates and algorithms, which form the foundation of gate-based qudit computation and equivalent approaches. Most gates and algorithms based on qudits have some advantage over those for qubits, such as shorter computational time, fewer resources, higher availability, and the ability to solve more complex problems. The qudit system, with its high-dimensional nature, can provide more degrees of freedom and larger computational space. Of course these advantages can come with challenges such as possibly harder-to-implement universal gates, benchmarking [142] and error correction connected with the complexity of the Clifford hierarchy for qudits [44].

Compared to qubit systems, qudit systems currently have received less attention in both theoretical and experimental studies. However, qudit quantum computing is becoming increasingly important as many topics and problems in this field are ripe for exploration. Extending from qubits to qudits ushes in some mathematical challenges, with these mathematical problems elegant and perhaps giving new insights into quantum computing in their own right. Connections between quantum resources such as entanglement, quantum algorithms and their improvements, scaling up qudit systems both to higher dimension and to more particles, benchmarking and error correction, and the bridging between qudits and continuous-variable quantum computing [42] are examples of the fantastic research directions in this field of high-dimensional quantum computing.

Author Contributions

All authors discussed the relevant materials to be added and all participated in writing the article.

Funding

We would like to acknowledge the financial support by the National Science Foundation under award number 1839191-ECCS. BCS appreciates financial support from NSERC and from the Alberta Government.

References

- [1] J.-L. Brylinski and R. Brylinski, “Universal quantum gates,” in *Mathematics of quantum computation*, pp. 117–134, Chapman and Hall/CRC, 2002.
- [2] H.-H. Lu, Z. Hu, M. S. Alshaykh, A. J. Moore, Y. Wang, P. Imany, A. M. Weiner, and S. Kais, “Quantum phase estimation with time-frequency qudits in a single photon,” *Advanced Quantum Technologies*, vol. 0, no. 0, p. 1900074, 2019.
- [3] M. Luo and X. Wang, “Universal quantum computation with qudits,” *Science China Physics, Mechanics & Astronomy*, vol. 57, pp. 1712–1717, Sep 2014.
- [4] B. Li, Z.-H. Yu, and S.-M. Fei, “Geometry of quantum computation with qutrits,” *Sci. Rep.*, vol. 3, p. 2594, 2013.
- [5] M.-X. Luo, X.-B. Chen, Y.-X. Yang, and X. Wang, “Geometry of quantum computation with qudits,” *Sci. Rep.*, vol. 4, p. 4044, 2014.
- [6] V. E. Zobov and A. S. Ermilov, “Implementation of a quantum adiabatic algorithm for factorization on two qudits,” *J. Exp. Theor. Phys.*, vol. 114, pp. 923–932, 07 2012.
- [7] M. H. Amin, N. G. Dickson, and P. Smith, “Adiabatic quantum optimization with qudits,” *Quantum Inf. Process.*, vol. 12, pp. 1819–1829, 04 2013.
- [8] S. X. Cui and Z. Wang, “Universal quantum computation with metaplectic anyons,” *J. Math. Phys.*, vol. 56, no. 3, p. 032202, 2015.
- [9] S. X. Cui, S.-M. Hong, and Z. Wang, “Universal quantum computation with weakly integral anyons,” *Quantum Information Processing*, vol. 14, no. 8, pp. 2687–2727, 2015.
- [10] A. Bocharov, S. X. Cui, M. Roetteler, and K. M. Svore, “Improved quantum ternary arithmetic,” *Quantum Info. Comput.*, vol. 16, p. 862884, July 2016.
- [11] X. Gao, M. Erhard, A. Zeilinger, and M. Krenn, “Computer-inspired concept for high-dimensional multipartite quantum gates,” *arXiv:1910.05677*, 2019.
- [12] S. D. Bartlett, H. de Guise, and B. C. Sanders, “Quantum encodings in spin systems and harmonic oscillators,” *Phys. Rev. A*, vol. 65, p. 052316, May 2002.
- [13] M. R. A. Adcock, P. Høyer, and B. C. Sanders, “Quantum computation with coherent spin states and the close Hadamard problem,” *Quantum Inf. Process.*, vol. 15, pp. 1361–1386, Jan 2016.

- [14] A. B. Klimov, R. Guzmán, J. C. Retamal, and C. Saavedra, “Qutrit quantum computer with trapped ions,” *Phys. Rev. A*, vol. 67, p. 062313, Jun 2003.
- [15] S. Dogra, Arvind, and K. Dorai, “Determining the parity of a permutation using an experimental nmr qutrit,” *Physics Letters A*, vol. 378, no. 46, pp. 3452 – 3456, 2014.
- [16] Z. Gedik, I. A. Silva, B. Lie akmak, G. Karpát, E. L. G. Vidoto, D. O. Soares-Pinto, E. R. deAzevedo, and F. F. Fanchini, “Computational speed-up with a single qudit,” *Sci. Rep.*, vol. 5, pp. 14671 EP –, Oct 2015. Article.
- [17] M. N. Leuenberger and D. Loss, “Quantum computing in molecular magnets,” *Nature*, vol. 410, no. 6830, p. 789, 2001.
- [18] M. Howard and J. Vala, “Qudit versions of the qubit $\pi/8$ gate,” *Phys. Rev. A*, vol. 86, p. 022316, Aug 2012.
- [19] J. Daboul, X. Wang, and B. C. Sanders, “Quantum gates on hybrid qudits,” *J. Phys. A.*, vol. 36, pp. 2525–2536, feb 2003.
- [20] J. C. Garcia-Escartin and P. Chamorro-Posada, “A swap gate for qudits,” *Quantum Inf. Process.*, vol. 12, pp. 3625–3631, Dec 2013.
- [21] T. C. Ralph, K. J. Resch, and A. Gilchrist, “Efficient Toffoli gates using qudits,” *Phys. Rev. A*, vol. 75, p. 022313, Feb 2007.
- [22] E. O. Kiktenko, A. S. Nikolaeva, P. Xu, G. V. Shlyapnikov, and A. K. Fedorov, “Scalable quantum computing with qudits on a graph,” *Phys. Rev. A*, vol. 101, p. 022304, Feb 2020.
- [23] D. M. Nguyen and S. Kim, “Quantum key distribution protocol based on modified generalization of Deutsch-Jozsa algorithm in d-level quantum system,” *International Journal of Theoretical Physics*, vol. 58, pp. 71–82, Jan 2019.
- [24] K. Nagata, H. Geurdes, S. K. Patro, S. Heidari, A. Farouk, and T. Nakamura, “Generalization of the BernsteinVazirani algorithm beyond qubit systems,” *Quantum Stud.: Math. Found.*, vol. 7, pp. 17–21, 03 2020.
- [25] Y. Cao, S.-G. Peng, C. Zheng, and G.-L. Long, “Quantum fourier transform and phase estimation in qudit system,” *Communications in Theoretical Physics*, vol. 55, pp. 790–794, may 2011.
- [26] A. Bocharov, M. Roetteler, and K. M. Svore, “Factoring with qutrits: Shor’s algorithm on ternary and metaplectic quantum architectures,” *Phys. Rev. A*, vol. 96, p. 012306, Jul 2017.

- [27] S. S. Ivanov, H. S. Tonchev, and N. V. Vitanov, “Time-efficient implementation of quantum search with qudits,” *Phys. Rev. A*, vol. 85, p. 062321, Jun 2012.
- [28] A. Y. Vlasov, “Noncommutative tori and universal sets of nonbinary quantum gates,” *J. Math. Phys.*, vol. 43, no. 6, pp. 2959–2964, 2002.
- [29] D. P. DiVincenzo, “Two-bit gates are universal for quantum computation,” *Phys. Rev. A*, vol. 51, no. 2, p. 1015, 1995.
- [30] D. Gottesman, “Fault-tolerant computation with higher-dimensional systems,” in *Lecture Notes in Computer Science* (W. C.P., ed.), vol. 1509 of *NASA International Conference on Quantum Computing and Quantum Communications*, pp. 302–313, Berlin: Springer, 1999.
- [31] D. L. Zhou, B. Zeng, Z. Xu, and C. P. Sun, “Quantum computation based on d -level cluster state,” *Phys. Rev. A*, vol. 68, p. 062303, Dec 2003.
- [32] S. S. Bullock, D. P. O’Leary, and G. K. Brennen, “Asymptotically optimal quantum circuits for d -level systems,” *Phys. Rev. Lett.*, vol. 94, p. 230502, Jun 2005.
- [33] W.-D. Li, Y.-J. Gu, K. Liu, Y.-H. Lee, and Y.-Z. Zhang, “Efficient universal quantum computation with auxiliary Hilbert space,” *Phys. Rev. A*, vol. 88, p. 034303, Sep 2013.
- [34] B. Mischuck and K. Mølmer, “Qudit quantum computation in the Jaynes-Cummings model,” *Phys. Rev. A*, vol. 87, p. 022341, Feb 2013.
- [35] M. Reck, A. Zeilinger, H. J. Bernstein, and P. Bertani, “Experimental realization of any discrete unitary operator,” *Phys. Rev. Lett.*, vol. 73, pp. 58–61, Jul 1994.
- [36] D. J. Rowe, B. C. Sanders, and H. de Guise, “Representations of the Weyl group and Wigner functions for $SU(3)$,” *J. Math. Phys.*, vol. 40, no. 7, pp. 3604–3615, 1999.
- [37] A. Muthukrishnan and C. R. Stroud, “Multivalued logic gates for quantum computation,” *Phys. Rev. A*, vol. 62, p. 052309, Oct 2000.
- [38] G. K. Brennen, D. P. O’Leary, and S. S. Bullock, “Criteria for exact qudit universality,” *Phys. Rev. A*, vol. 71, p. 052318, May 2005.
- [39] D. Gottesman, “Theory of fault-tolerant quantum computation,” *Phys. Rev. A*, vol. 57, pp. 127–137, Jan 1998.
- [40] P. Boykin, T. Mor, M. Pulver, V. Roychowdhury, and F. Vatan, “A new universal and fault-tolerant quantum basis,” *Information Processing Letters*, vol. 75, no. 3, pp. 101 – 107, 2000.

- [41] J. Patera and H. Zassenhaus, “The Pauli matrices in n dimensions and finest gradings of simple lie algebras of type A_{n-1} ,” *J. Math. Phys.*, vol. 29, no. 3, pp. 665–673, 1988.
- [42] D. Gottesman, A. Kitaev, and J. Preskill, “Encoding a qubit in an oscillator,” *Phys. Rev. A*, vol. 64, no. 1, p. 012310, 2001.
- [43] M. A. Nielsen, M. J. Bremner, J. L. Dodd, A. M. Childs, and C. M. Dawson, “Universal simulation of hamiltonian dynamics for quantum systems with finite-dimensional state spaces,” *Phys. Rev. A*, vol. 66, p. 022317, Aug 2002.
- [44] Z. Webb, “The Clifford group forms a unitary 3-design,” *Quantum Inf. Comput.*, vol. 16, no. 15&16, pp. 1379–1400, 2016.
- [45] D. Gottesman and I. L. Chuang, “Demonstrating the viability of universal quantum computation using teleportation and single-qubit operations,” *Nature*, vol. 402, no. 6760, pp. 390–393, 1999.
- [46] B. Eastin and E. Knill, “Restrictions on transversal encoded quantum gate sets,” *Phys. Rev. Lett.*, vol. 102, p. 110502, Mar 2009.
- [47] B. Zeng, H. Chung, A. W. Cross, and I. L. Chuang, “Local unitary versus local Clifford equivalence of stabilizer and graph states,” *Phys. Rev. A*, vol. 75, p. 032325, Mar 2007.
- [48] R. A. Low, “Learning and testing algorithms for the Clifford group,” *Phys. Rev. A*, vol. 80, p. 052314, Nov 2009.
- [49] A. M. Childs, “Secure assisted quantum computation,” *arXiv:quant-ph/0111046*, 2001.
- [50] W. van Dam and M. Howard, “Noise thresholds for higher-dimensional systems using the discrete wigner function,” *Phys. Rev. A*, vol. 83, p. 032310, Mar 2011.
- [51] H. Anwar, E. T. Campbell, and D. E. Browne, “Qutrit magic state distillation,” *New Journal of Physics*, vol. 14, p. 063006, jun 2012.
- [52] E. T. Campbell, H. Anwar, and D. E. Browne, “Magic-state distillation in all prime dimensions using quantum Reed-Muller codes,” *Phys. Rev. X*, vol. 2, p. 041021, Dec 2012.
- [53] C. M. Wilmott, “On swapping the states of two qudits,” *Int. J. Quantum Inf.*, vol. 09, no. 06, pp. 1511–1517, 2011.
- [54] C. M. Wilmott and P. R. Wild, “On a generalized quantum swap gate,” *Int. J. Quantum Inf.*, vol. 10, no. 03, p. 1250034, 2012.
- [55] N. D. Mermin, “From classical state swapping to quantum teleportation,” *Phys. Rev. A*, vol. 65, p. 012320, Dec 2001.

- [56] K. Fujii, “Exchange gate on the qudit space and fock space,” *J. Opt. B*, vol. 5, pp. S613–S618, oct 2003.
- [57] G. A. Paz-Silva, S. Rebić, J. Twamley, and T. Duty, “Perfect mirror transport protocol with higher dimensional quantum chains,” *Phys. Rev. Lett.*, vol. 102, p. 020503, Jan 2009.
- [58] X. Wang, “Continuous-variable and hybrid quantum gates,” *J. Phys. A*, vol. 34, pp. 9577–9584, oct 2001.
- [59] G. Alber, A. Delgado, N. Gisin, and I. Jex, “Efficient bipartite quantum state purification in arbitrary dimensional Hilbert spaces,” *J. Phys. A*, vol. 34, pp. 8821–8833, oct 2001.
- [60] A. M. C. R. Stroud, “Quantum fast fourier transform using multilevel atoms,” *J. Mod. Opt.*, vol. 49, no. 13, pp. 2115–2127, 2002.
- [61] D. G. Cory, M. D. Price, W. Maas, E. Knill, R. Laflamme, W. H. Zurek, T. F. Havel, and S. S. Somaroo, “Experimental quantum error correction,” *Phys. Rev. Lett.*, vol. 81, pp. 2152–2155, Sep 1998.
- [62] E. Dennis, “Toward fault-tolerant quantum computation without concatenation,” *Phys. Rev. A*, vol. 63, p. 052314, Apr 2001.
- [63] Y. Shi, “Both Toffoli and controlled-NOT need little help to do universal quantum computation,” *arXiv preprint quant-ph/0205115*, 2002.
- [64] B. P. Lanyon, M. Barbieri, M. P. Almeida, T. Jennewein, T. C. Ralph, K. J. Resch, G. J. Pryde, J. L. O’Hara, H. M. Heffern, A. Gilchrist, and A. G. White, “Simplifying quantum logic using higher-dimensional Hilbert spaces,” *Nature Physics*, vol. 5, no. 2, pp. 134–140, 2009.
- [65] M. A. Nielsen and I. L. Chuang, *Quantum Computation and Quantum Information: 10th Anniversary Edition*. New York, NY, USA: Cambridge University Press, 10th ed., 2011.
- [66] A. Aspuru-Guzik, A. D. Dutoi, P. J. Love, and M. Head-Gordon, “Simulated quantum computation of molecular energies,” *Science*, vol. 309, no. 5741, pp. 1704–1707, 2005.
- [67] P. W. Shor, “Algorithms for quantum computation: discrete logarithms and factoring,” in *Proceedings 35th Annual Symposium on Foundations of Computer Science*, pp. 124–134, Nov 1994.
- [68] R. Cleve, A. Ekert, C. Macchiavello, and M. Mosca, “Quantum algorithms revisited,” *Proceedings of the Royal Society of London. Series A: Mathematical, Physical and Engineering Sciences*, vol. 454, no. 1969, pp. 339–354, 1998.
- [69] Y.-M. Di and H.-R. Wei, “Synthesis of multivalued quantum logic circuits by elementary gates,” *Phys. Rev. A*, vol. 87, p. 012325, Jan 2013.

- [70] F. S. Khan and M. Perkowski, “Synthesis of multi-qudit hybrid and d-valued quantum logic circuits by decomposition,” *Theor. Comput. Sci.*, vol. 367, no. 3, pp. 336 – 346, 2006.
- [71] M. A. Nielsen, M. R. Dowling, M. Gu, and A. C. Doherty, “Quantum computation as geometry,” *Science*, vol. 311, no. 5764, pp. 1133–1135, 2006.
- [72] M. A. Nielsen, “A geometric approach to quantum circuit lower bounds,” *arXiv preprint quant-ph/0502070*, 2005.
- [73] D. Deutsch, “Quantum theory, the Church–Turing principle and the universal quantum computer,” *J. Phys. A*, vol. 400, no. 1818, pp. 97–117, 1985.
- [74] D. P. Deutsch and R. Jozsa, “Rapid solution of problems by quantum computation,” *Proc. Royal Soc. Lond. A*, vol. 439, pp. 553–558, 1992.
- [75] M. Van den Nest, “Universal quantum computation with little entanglement,” *Phys. Rev. Lett.*, vol. 110, p. 060504, Feb 2013.
- [76] M. Howard, J. Wallman, V. Veitch, and J. Emerson, “Contextuality supplies the ‘magic’ for quantum computation,” *Nature*, vol. 510, p. 351, Jun 2014. Article.
- [77] S. Kochen and E. P. Specker, *The Problem of Hidden Variables in Quantum Mechanics*, pp. 293–328. Dordrecht: Springer Netherlands, 1975.
- [78] A. A. Klyachko, M. A. Can, S. Binicioğlu, and A. S. Shumovsky, “Simple test for hidden variables in spin-1 systems,” *Phys. Rev. Lett.*, vol. 101, p. 020403, Jul 2008.
- [79] X. Zhan, J. Li, H. Qin, Z. hao Bian, and P. Xue, “Linear optical demonstration of quantum speed-up with a single qudit,” *Opt. Express*, vol. 23, pp. 18422–18427, Jul 2015.
- [80] Y. Fan, “A generalization of the Deutsch-Jozsa algorithm to multi-valued quantum logic,” in *37th International Symposium on Multiple-Valued Logic (ISMVL’07)*, pp. 12–12, May 2007.
- [81] E. Kiktenko, A. Fedorov, A. Strakhov, and V. Man’ko, “Single qudit realization of the Deutsch algorithm using superconducting many-level quantum circuits,” *Physics Letters A*, vol. 379, no. 22, pp. 1409 – 1413, 2015.
- [82] A. R. Kessel and N. M. Yakovleva, “Implementation schemes in NMR of quantum processors and the Deutsch-Jozsa algorithm by using virtual spin representation,” *Phys. Rev. A*, vol. 66, p. 062322, Dec 2002.
- [83] E. Bernstein and U. Vazirani, “Quantum complexity theory,” *SIAM Journal on Computing*, vol. 26, no. 5, pp. 1411–1473, 1997.

- [84] R. Krishna, V. Makwana, and A. P. Suresh, “A generalization of Bernstein-Vazirani algorithm to qudit systems,” *arXiv preprint arXiv:1609.03185*, 2016.
- [85] Z. Zilic and K. Radecka, “Scaling and better approximating quantum Fourier transform by higher radices,” *IEEE Transactions on Computers*, vol. 56, pp. 202–207, Feb 2007.
- [86] D. Coppersmith, “An approximate Fourier transform useful in quantum factoring,” *arXiv preprint quant-ph/0201067*, 2002.
- [87] V. V. Shende, S. S. Bullock, and I. L. Markov, “Synthesis of quantum-logic circuits,” *IEEE Transactions on Computer-Aided Design of Integrated Circuits and Systems*, vol. 25, pp. 1000–1010, June 2006.
- [88] V. Parasa and M. Perkowski, “Quantum phase estimation using multi-valued logic,” in *2011 41st IEEE International Symposium on Multiple-Valued Logic*, pp. 224–229, May 2011.
- [89] D. S. Abrams and S. Lloyd, “Quantum algorithm providing exponential speed increase for finding eigenvalues and eigenvectors,” *Phys. Rev. Lett.*, vol. 83, pp. 5162–5165, Dec 1999.
- [90] A. W. Harrow, A. Hassidim, and S. Lloyd, “Quantum algorithm for linear systems of equations,” *Phys. Rev. Lett.*, vol. 103, p. 150502, Oct 2009.
- [91] J. Pan, Y. Cao, X. Yao, Z. Li, C. Ju, H. Chen, X. Peng, S. Kais, and J. Du, “Experimental realization of quantum algorithm for solving linear systems of equations,” *Physical Review A*, vol. 89, no. 2, p. 022313, 2014.
- [92] H. S. Tonchev and N. V. Vitanov, “Quantum phase estimation and quantum counting with qudits,” *Phys. Rev. A*, vol. 94, p. 042307, Oct 2016.
- [93] H. Wang, S. Kais, A. Aspuru-Guzik, and M. R. Hoffmann, “Quantum algorithm for obtaining the energy spectrum of molecular systems,” *Phys. Chem. Chem. Phys.*, vol. 10, pp. 5388–5393, 2008.
- [94] H. Wang, S. Kais, A. Aspuru-Guzik, and M. R. Hoffmann, “Quantum algorithm for obtaining the energy spectrum of molecular systems,” *Physical Chemistry Chemical Physics*, vol. 10, no. 35, pp. 5388–5393, 2008.
- [95] A. Daskin and S. Kais, “Decomposition of unitary matrices for finding quantum circuits: application to molecular hamiltonians,” *The Journal of chemical physics*, vol. 134, no. 14, p. 144112, 2011.
- [96] A. Daskin, A. Grama, G. Kollias, and S. Kais, “Universal programmable quantum circuit schemes to emulate an operator,” *The Journal of chemical physics*, vol. 137, no. 23, p. 234112, 2012.
- [97] S. Kais, “Introduction to quantum information and computation for chemistry,” *Quantum Inf. Comput. Chem*, vol. 154, pp. 1–38, 2014.

- [98] T. Bian, D. Murphy, R. Xia, A. Daskin, and S. Kais, “Quantum computing methods for electronic states of the water molecule,” *Molecular Physics*, vol. 117, no. 15-16, pp. 2069–2082, 2019.
- [99] M. Sawerwain and W. Leoński, “Quantum circuits based on qutrits as a tool for solving systems of linear equations,” *arXiv:1309.0800*, 2013.
- [100] P. W. Shor, “Polynomial-time algorithms for prime factorization and discrete logarithms on a quantum computer,” *SIAM review*, vol. 41, no. 2, pp. 303–332, 1999.
- [101] Y. Fan, “Applications of multi-valued quantum algorithms,” *arXiv:0809.0932*, 2008.
- [102] H. Li, C. Wu, W. Liu, P. Chen, and C. Li, “Fast quantum search algorithm for databases of arbitrary size and its implementation in a cavity QED system,” *Physics Letters A*, vol. 375, no. 48, pp. 4249 – 4254, 2011.
- [103] J. R. Morris and B. W. Shore, “Reduction of degenerate two-level excitation to independent two-state systems,” *Phys. Rev. A*, vol. 27, pp. 906–912, Feb 1983.
- [104] E. S. Kyoseva and N. V. Vitanov, “Coherent pulsed excitation of degenerate multistate systems: Exact analytic solutions,” *Phys. Rev. A*, vol. 73, p. 023420, Feb 2006.
- [105] F. Jelezko, T. Gaebel, I. Popa, M. Domhan, A. Gruber, and J. Wrachtrup, “Observation of coherent oscillation of a single nuclear spin and realization of a two-qubit conditional quantum gate,” *Phys. Rev. Lett.*, vol. 93, p. 130501, Sep 2004.
- [106] L. Childress, M. V. Gurudev Dutt, J. M. Taylor, A. S. Zibrov, F. Jelezko, J. Wrachtrup, P. R. Hemmer, and M. D. Lukin, “Coherent dynamics of coupled electron and nuclear spin qubits in diamond,” *Science*, vol. 314, no. 5797, pp. 281–285, 2006.
- [107] P. Neumann, J. Beck, M. Steiner, F. Rempp, H. Fedder, P. R. Hemmer, J. Wrachtrup, and F. Jelezko, “Single-shot readout of a single nuclear spin,” *Science*, vol. 329, no. 5991, pp. 542–544, 2010.
- [108] D. Loss and D. P. DiVincenzo, “Quantum computation with quantum dots,” *Phys. Rev. A*, vol. 57, pp. 120–126, Jan 1998.
- [109] K. C. Nowack, F. H. L. Koppens, Y. V. Nazarov, and L. M. K. Vandersypen, “Coherent control of a single electron spin with electric fields,” *Science*, vol. 318, no. 5855, pp. 1430–1433, 2007.
- [110] G. J. Milburn, “Photons as qubits,” *Physica Scripta*, vol. T137, p. 014003, dec 2009.

- [111] R. Prevedel, P. Walther, F. Tiefenbacher, P. BMei hi, R. Kaltenbaek, T. Jennewein, and A. Zeilinger, “High-speed linear optics quantum computing using active feed-forward,” *Nature*, vol. 445, no. 7123, pp. 65–69, 2007.
- [112] I. Chiorescu, Y. Nakamura, C. J. P. M. Harmans, and J. E. Mooij, “Coherent quantum dynamics of a superconducting flux qubit,” *Science*, vol. 299, no. 5614, pp. 1869–1871, 2003.
- [113] J. Clarke and F. K. Wilhelm, “Superconducting quantum bits,” *Nature*, vol. 453, no. 7198, pp. 1031–1042, 2008.
- [114] R. Blatt and D. Wineland, “Entangled states of trapped atomic ions,” *Nature*, vol. 453, no. 7198, pp. 1008–1015, 2008.
- [115] I. Bloch, “Quantum coherence and entanglement with ultracold atoms in optical lattices,” *Nature*, vol. 453, no. 7198, pp. 1016–1022, 2008.
- [116] F. Troiani and M. Affronte, “Molecular spins for quantum information technologies,” *Chemical Society Reviews*, vol. 40, no. 6, pp. 3119–3129, 2011.
- [117] L. Bogani and W. Wernsdorfer, “Molecular spintronics using single-molecule magnets,” in *Nanoscience And Technology: A Collection of Reviews from Nature Journals*, pp. 194–201, World Scientific, 2010.
- [118] J. M. Clemente-Juan, E. Coronado, and A. Gaita-Ariño, “Magnetic polyoxometalates: from molecular magnetism to molecular spintronics and quantum computing,” *Chemical Society Reviews*, vol. 41, no. 22, pp. 7464–7478, 2012.
- [119] G. Aromí, D. Aguila, P. Gamez, F. Luis, and O. Roubeau, “Design of magnetic coordination complexes for quantum computing,” *Chemical Society Reviews*, vol. 41, no. 2, pp. 537–546, 2012.
- [120] I. L. Chuang, L. M. Vandersypen, X. Zhou, D. W. Leung, and S. Lloyd, “Experimental realization of a quantum algorithm,” *Nature*, vol. 393, no. 6681, p. 143, 1998.
- [121] L. M. Vandersypen, M. Steffen, G. Breyta, C. S. Yannoni, M. H. Sherwood, and I. L. Chuang, “Experimental realization of Shor’s quantum factoring algorithm using nuclear magnetic resonance,” *Nature*, vol. 414, no. 6866, p. 883, 2001.
- [122] E. Moreno-Pineda, C. Godfrin, F. Balestro, W. Wernsdorfer, and M. Ruben, “Molecular spin qubits for quantum algorithms,” *Chem. Soc. Rev.*, vol. 47, pp. 501–513, 2018.
- [123] A. Babazadeh, M. Erhard, F. Wang, M. Malik, R. Nouroozi, M. Krenn, and A. Zeilinger, “High-dimensional single-photon quantum gates: Concepts and experiments,” *Phys. Rev. Lett.*, vol. 119, p. 180510, Nov 2017.

- [124] M. Erhard, R. Fickler, M. Krenn, and A. Zeilinger, “Twisted photons: new quantum perspectives in high dimensions,” *Light Sci. Appl.*, vol. 7, p. 17146, 2018.
- [125] M. Kues, C. Reimer, P. Roztocki, L. Romero Corts, S. Sciara, B. Wetzl, Y. Zhang, A. Cino, S. T. Chu, B. E. Little, D. J. Moss, L. Caspani, J. Azaña, and R. Morandotti, “On-chip generation of high-dimensional entangled quantum states and their coherent control,” *Nature*, vol. 546, no. 6760, pp. 622–626, 2017.
- [126] H.-H. Lu, J. M. Lukens, N. A. Peters, O. D. Odele, D. E. Leaird, A. M. Weiner, and P. Lougovski, “Electro-optic frequency beam splitters and tritters for high-fidelity photonic quantum inf. process.,” *Phys. Rev. Lett.*, vol. 120, no. 3, p. 030502, 2018.
- [127] P. Imany, J. A. Jaramillo-Villegas, O. D. Odele, K. Han, D. E. Leaird, J. M. Lukens, P. Lougovski, M. Qi, and A. M. Weiner, “50-ghz-spaced comb of high-dimensional frequency-bin entangled photons from an on-chip silicon nitride microresonator,” *Opt. Express*, vol. 26, no. 2, pp. 1825–1840, 2018.
- [128] P. Imany, J. A. Jaramillo-Villegas, M. S. Alshaykh, J. M. Lukens, O. D. Odele, A. J. Moore, D. E. Leaird, M. Qi, and A. M. Weiner, “High-dimensional optical quantum logic in large operational spaces,” *npj Quantum Inf.*, vol. 5, Jul 2019.
- [129] N. T. Islam, C. C. W. Lim, C. Cahall, J. Kim, and D. J. Gauthier, “Provably secure and high-rate quantum key distribution with time-bin qudits,” *Science advances*, vol. 3, no. 11, p. e1701491, 2017.
- [130] P. C. Humphreys, B. J. Metcalf, J. B. Spring, M. Moore, X.-M. Jin, M. Barbieri, W. S. Kolthammer, and I. A. Walmsley, “Linear optical quantum computing in a single spatial mode,” *Phys. Rev. Lett.*, vol. 111, p. 150501, Oct 2013.
- [131] D. Mc Hugh and J. Twamley, “Trapped-ion qutrit spin molecule quantum computer,” *New J. Phys.*, vol. 7, no. 1, p. 174, 2005.
- [132] F. A. Bovey, P. A. Mirau, and H. Gutowsky, *Nuclear magnetic resonance spectroscopy*. Elsevier, 1988.
- [133] C. P. Slichter, *Principles of magnetic resonance*, vol. 1. Springer Science & Business Media, 2013.
- [134] J.-S. Lee and A. K. Khitrin, “Projective measurement in nuclear magnetic resonance,” *Applied physics letters*, vol. 89, no. 7, p. 074105, 2006.
- [135] E. Moreno Pineda, T. Komeda, K. Katoh, M. Yamashita, and M. Ruben, “Surface confinement of TbPc2-SMMs: structural, electronic and magnetic properties,” *Dalton Trans.*, vol. 45, pp. 18417–18433, 2016.

- [136] M. Urdampilleta, S. Klyatskaya, J.-P. Cleuziou, M. Ruben, and W. Wernsdorfer, “Supramolecular spin valves,” *Nature materials*, vol. 10, no. 7, p. 502, 2011.
- [137] M. Ganzhorn, S. Klyatskaya, M. Ruben, and W. Wernsdorfer, “Strong spin–phonon coupling between a single-molecule magnet and a carbon nanotube nanoelectromechanical system,” *Nat. Nanotechnol.*, vol. 8, no. 3, p. 165, 2013.
- [138] S. Thiele, F. Balestro, R. Ballou, S. Klyatskaya, M. Ruben, and W. Wernsdorfer, “Electrically driven nuclear spin resonance in single-molecule magnets,” *Science*, vol. 344, no. 6188, pp. 1135–1138, 2014.
- [139] N. Ishikawa, M. Sugita, T. Okubo, N. Tanaka, T. Iino, and Y. Kaizu, “Determination of ligand-field parameters and f-electronic structures of double-decker bis (phthalocyaninato) lanthanide complexes,” *Inorganic chemistry*, vol. 42, no. 7, pp. 2440–2446, 2003.
- [140] C. Godfrin, A. Ferhat, R. Ballou, S. Klyatskaya, M. Ruben, W. Wernsdorfer, and F. Balestro, “Operating quantum states in single magnetic molecules: implementation of grovers quantum algorithm,” *Phys. Rev. Lett.*, vol. 119, no. 18, p. 187702, 2017.
- [141] D. P. DiVincenzo, “The physical implementation of quantum computation,” *Fortschritte der Physik: Progress of Physics*, vol. 48, no. 9-11, pp. 771–783, 2000.
- [142] M. Jafarzadeh, Y.-D. Wu, Y. R. Sanders, and B. C. Sanders, “Randomized benchmarking for qudit Clifford gates,” *New J. Phys.*, vol. 22, p. 063014, 06 2020.